www.sciencemag.org/cgi/content/full/330/6008/1251/DC1

# Supporting Online Material for

## Reprogramming Cellular Behavior with RNA Controllers Responsive to Endogenous Proteins

Stephanie J. Culler, Kevin G. Hoff, Christina D. Smolke*

*To whom correspondence should be addressed. E-mail: csmolke@stanford.edu

Published 26 November 2010, *Science* **330**, 1251 (2010)
DOI: 10.1126/science.1192128

**This PDF file includes:**

## Materials and Methods

### Construction of RNA device plasmids

The SMN1-GFP mini-gene fusion plasmid (pCS1773) was constructed through PCR amplification, digestion and ligation in the appropriate expression vector. A region encompassing the last nine nucleotides of exons 6 through the first 21 nucleotides of exon 8 of the *SMN1* mini-gene (*S1*) was amplified through PCR from template pCS1774 with primers Ex6 and Ex8 and PfuUltra II fusion high-fidelity DNA polymerase (Stratagene) and the resulting PCR product was digested with NheI. The *SMN1* mini-gene DNA synthesis was performed by DNA 2.0 to contain restriction sites KpnI, EcoRV, ClaI (positions -87, -61 and -50 from 3' ss of exon 7, respectively) and XhoI, HindIII, BamHI and XbaI (positions +10, +50, +70 and +97 from 5' ss of exon 7, respectively). The *GFP* gene was amplified from the template pKW430 (*S2*) with primers GFP1 and GFP2. The resulting PCR product was digested with ApaI and NheI and ligated into the corresponding restriction sites of the mammalian expression vector pcDNA5/FRT (Invitrogen). The *SMN1* mini-gene PCR product was then ligated into the NheI restriction site of the resulting GFP construct, to construct the base plasmid SMN1-GFP. The aptamer sequences used in this study are CGTACACCATCAGGGTACG (*S3*) for MS2; CGTACCCATCAGGGTACG (lacks a bulged adenosine required for MS2 binding) (*S3, S4*) for MS2Δ; AGGCCGATCTATGGACGCTATAGGCACACCGGATACTTTAACGATTGGCT (*S5*) for β-catenin; TCGGTTAGCAATTTCATAGGCCACACGGATATCGCAGGTATCTAGC CGGA (reverse compliment) for β-cateninΔ; GCATCCTGAAACTGTTTTAAGGTTGGCCGA TGC (*S6*) for NF-κB p50(1); CGTAGCCGGTTGGAATTTTGTCAAAGTCCTACG (reverse compliment) for NF-κB p50(1)Δ and p50(2)Δ; GATCTTGAAACTGTTTTAAGGTTGGCCGA TC (*S7*) for NF-κB p50(2); GAAGCTTACAAGAAGGACAGCACGAATAAAACCTGCGTAA ATCCGCCCCATTTGTGTAAGGGTAGTGGGTCGAATTCCGCTCA (*S8*) for NF-κB p65;

ACTCGCCTTAAGCTGGGTGATGGGAATGTGTTTACCCCGCCTAAATGCGTCCAAAAT AAGCACGACAGGAAGAACATTCGAAG (reverse compliment) for NF-κB p65Δ.

Aptamer and mutant cassette sequences containing portions of the *SMN1* mini-gene were digested and ligated into the appropriate restriction sites within the SMN1-GFP plasmid (Table S8). Briefly, oligonucleotides encoding the forward and reverse strands of the wild-type and mutant MS2 coat protein aptamers were annealed, digested with the appropriate restriction enzymes and ligated into SMN1-GFP. β-catenin aptamer constructs were generated through PCR using the oligonucleotide cassette templates β-cat-3, β-catΔ-3, β-cat-6, and β-catΔ-6 (Table S9) and reverse primer AptRv with forward primers Bcat3, BcatΔ3, Bcat6, and BcatΔ6, respectively (Table S7). Similarly, for the NF-κB p50 and p65 aptamer constructs, the oligonucleotide cassette templates NF-κBp50(1)-3, NF-κBp50(1)Δ-3, NF-κBp50(2)-3, NF-κBp65-3, and NF-κBp65Δ-3 were PCR amplified with reverse primer AptRv and forward primers p50(1), p50(1)Δ, p50(2), and p65, respectively. The resulting β-catenin, NF-κB p50 and p65 wild-type and mutant PCR products were digested with the appropriate restriction enzymes and ligated into the corresponding restriction sites of SMN1-GFP (pCS1775-pCS1783, Table S8). To construct the multi-input RNA devices containing the wild-type and mutant MS2 coat protein aptamers in positions 3 and 10, the MS2-3 and MS2Δ-3 annealed cassettes were digested with EcoRV and XhoI and ligated into the corresponding restriction sites of SMN1-GFP containing the wild-type and mutant MS2 coat protein aptamers in position 10 (pCS1784-pCS1787, Table S8). To construct the multi-input RNA devices containing the wild-type and mutant NF-κB p65 aptamers in position 3 and the wild-type and mutant MS2 coat protein aptamers, the NF-κB p65 PCR products were digested with EcoRV and Xho I and ligated into the corresponding restriction sites

of SMN1-GFP containing the wild-type and mutant MS2 coat protein aptamers in position 10 (pCS1788-pCS1791, Table S8).

The SMN1-Puma and SMN1-TK fusion plasmids were constructed in two steps. The human *Puma* gene was amplified from pORF5-hPUMA (Invivogen) with primers Puma1 and Puma2 designed to place a flexible Gly-Ser linker (GGSGGS) at the 5' end of the gene. The resulting PCR product was digested with NheI and PmeI and ligated into the corresponding restriction sites of pcDNA5/FRT to construct the plasmid pCS1792. The SMN1-GFP constructs pCS1793-pCS1794, pCS1777-pCS1778, pCS1782-pCS1783 were digested with NheI and the resulting *SMN1* mini-genes were ligated into the corresponding restriction site in pCS1773, resulting in plasmids MS2-3-Puma, MS2Δ-3-Puma, β-cat-6-Puma, β-catΔ-6-Puma, p65-3-Puma, and p65Δ-3-Puma (pCS1795-pCS1800, Table S8). Similarly, to construct the SMN1-TK plasmids the *HSV-TK* gene was amplified from pCD19t-Tk-T2A-IL15op_epHIV7 (a generous gift from M. Jensen, City of Hope) using primers TK1 and TK2. The resulting PCR product was digested with NheI and PmeI and ligated into corresponding restriction sites of pcDNA5/FRT creating pCS1801. The NheI digested *SMN1* mini-genes from pCS1777-pCS1778 and pCS1782-pCS1783 were ligated into the corresponding restriction site of pCS1801, resulting in plasmids β-cat-6-TK, β-catΔ-6-TK, p65-3-TK, and p65Δ-3-TK (pCS1802-pCS1805, Table S8).

To construct the MS2-DsRed expression plasmid (pCS1392), the *DsRed* monomer gene was amplified from pDsRed-monomer (Clontech) with primers DsRed1 and DsRed2, digested with BamHI and NotI and ligated into the corresponding restriction sites of pcDNA5/FRT creating pCS489. The MS2 coat protein gene was amplified in two steps from template pHis-BIVT-MS2-RSp55 (*S9*) using primers MS2-1 and MS2-2 for the first round and MS2-3 and MS2-2 for the second round to fuse a FLAG epitope (DYKDDDDK) (*S10*) followed by an SV40

NLS (PKKKRKV) (*S11*), to the 5' end of the MS2 coat protein gene. The final PCR product was digested with KpnI and BamHI and ligated into the corresponding restriction sites of pCS489. The p50-DsRed expression plasmid (pCS1806) was constructed similarly, where the *p50* gene was amplified in two steps from template pGAD424 (*S12*) using primers p50-1 and p50-2 for the first round and p50-3 and p50-2 for the second round to fuse a FLAG epitope followed by a SV40 NLS to the 5' end of the *p50* gene. The final PCR product was digested with NheI and KpnI and ligated into the corresponding restriction sites pCS489.

To construct the MS2-Venus expression plasmid (pCS1806), the construct pCS2/Venus (*S13*) was digested with BamHI and ApaI and the resulting *venus* gene was ligated into the corresponding restriction sites of pcDNA5/FRT creating pCS1807. pCS1392 was digested with KpnI and BamHI and the resulting FLAG-NLS-MS2 fragment was ligated into the corresponding restriction sites of pCS1807. Venus was chosen as our fluorescent reporter for the MS2 induced apoptosis studies (Fig. S5A and B) to avoid significant spectral overlap with the 7-aminoactinomycin D (7AAD) viability dye.

**Cell culture, transfections, stable cell lines, and flow cytometry analysis**

All cell culture media was obtained from Invitrogen. Isogenic HEK-293 stable cell lines were generated by co-transfection of the appropriate RNA device construct and a plasmid encoding the Flp recombinase (pOG44) in HEK-293 FLP-In cells grown in medium without Zeocin according to the manufacturer's instructions (Invitrogen). Stable selections were carried out in 6-well plates seeded with ~$2x10^5$ HEK-293 FLP-In cells per well, where 1.8 µg of pOG44 and .2 µg of the RNA device construct (10:1 ratio) were co-transfected. Fresh medium was added to the cells 24 h after transfection. The cells were expanded by a 1:4 dilution and Hygromycin B was

added to a final concentration of 200 μg/ml 48 h after transfection. Clones were harvested by trypsinization, pooled, and analyzed using a Quanta Cell Lab Cytometer (Beckman Coulter; Fullerton, CA) 10-14 days after transfection. Flow cytometry data was analyzed using the FlowJo v.7.1 (Tree Star, Inc.) software package. Flow cytometry analysis and gating procedures for all regulatory devices is presented in Figs. S6 to S9.

For transient transfection studies, HEK-293 cell lines stably expressing the RNA devices were seeded in 24-well plates at ~$5x10^4$ cells per well 16 to 24 h prior to transfection. Cell lines were transfected with 250 ng of the appropriate MS2-DsRed, MS2-Venus, p50-DsRed, DsRed, or Venus expression constructs. The cells were harvested by trypsinization, pooled, and analyzed by flow cytometry and microscopy 48 h after transfection. All presented microscopy images were taken during an individual experiment. GFP and DsRed fluorescence, as measured by flow cytometry, was excited at 488 nm and emission was measured through a 525-nm filter and a 610-nm band-pass filter, respectively. Experiments were carried out on different days and transfections were completed in duplicate, where the mean GFP fluorescence of the DsRed viable transfected population was evaluated. GFP fluorescence levels of both the wild-type and mutant RNA devices in the presence of ligand were normalized to the GFP fluorescence of the cell lines in the absence of ligand. Relative expression (fold) data is reported as the normalized mean fluorescence for each wild-type sample divided by the normalized mean fluorescence for each mutant sample $\pm$ the average error.

For the induction of the Wnt and NF-κB pathways, HEK-293 cell lines stably expressing the RNA devices were seeded in a 24-well plate at ~$5x10^4$ cells per well 16 to 24 h prior to induction with $LTD_4$ or TNF-α. Cells were treated with 20 ng/mL TNF-α (Sigma) for 48 h for the NF-κB pathway induction studies (*S14*). For the Wnt pathway induction studies, cells were

serum starved 2 h before stimulation with 80 nM leukotriene $D_4$ ($LTD_4$) (Sigma) for 48 h in the absence of serum (*S15*). After stimulation of either pathway, the cells were harvested by trypsinization, pooled and analyzed by flow cytometry and microscopy. GFP fluorescence as measured by flow cytometry was excited at 488 nm and emission was measured through a 525-nm filter band-pass filter. Both microscopy and flow cytometry experiments were carried out on different days and were completed in duplicate, where the mean GFP fluorescence of the viable cell population and the average error between samples is reported. GFP fluorescence levels of both the wild-type and mutant RNA devices in the presence of ligand were normalized to the GFP fluorescence of the cell lines in the absence of ligand. Relative expression (fold) data is reported as the normalized mean fluorescence for each wild-type sample divided by the normalized mean fluorescence for each mutant sample $\pm$ the average error.

**Apoptosis assays**

Stable cell lines were harvested by trypsinization as described above. For the Puma apoptosis studies, cell lines stably expressing the RNA devices were seeded in a 24-well plate at ~$5x10^4$ cells per well 16 to 24 h prior to induction with $LTD_4$ or TNF-α or transfection with 250 ng of MS2-Venus or Venus alone as described above. 48 h after transfection or induction, the pooled cells were washed in cold phosphate-buffered saline (PBS). Cells were stained with Pacific blue annexin V and 7AAD using the Vybrant Apoptosis Assay Kit (Invitrogen) according to the manufacturer's instructions. The fluorescence of the stained cells was measured using a Quanta Cell Lab Cytometer, where the Pacific blue dye was excited using a UV light source and measured through a 465/430 band-pass filter (FL1). Venus and 7AAD were excited with a 488-nm laser and measured through a 535-nm band-pass (FL2) and 670-nm long pass filter (FL3)

respectively. In this assay, live cells are annexin V negative and 7AAD negative, apoptotic cells are annexin V positive and 7AAD negative and dead cells are annexin V negative and 7AAD positive. Experiments were carried out on different days and transfections/inductions were completed in duplicate. For the MS2-Puma device studies the mean percentage of cells undergoing apoptosis (annexin V positive and 7AAD negative) within the Venus positive population $\pm$ the average error is reported. For the NF-κB and Wnt signaling devices fused to *Puma*, the mean percentage of cells undergoing apoptosis (annexin V positive and 7AAD negative) $\pm$ the average error is reported. Flow cytometry analysis and gating procedures for all apoptosis-inducing regulatory devices is presented in Figs. S8 and S9.

For the ganciclovir (GCV) sensitivity assays, HEK-293 cell lines stably expressing the RNA devices were seeded in a 24-well plate at ~$5x10^4$ cells per well 16 to 24 h prior to induction with $LTD_4$ or TNF-α. At the time of induction cells were either left untreated or incubated with different concentrations of GCV (10 or 100 μg/ml). After 96 h the cells were harvested by trypsinization, pooled and analyzed by flow cytometry and microscopy. For these studies, the mean percentage of alive cells (7AAD negative) $\pm$ the average error is reported.

**qRT-PCR analysis**

Total cellular RNA was purified from stably transfected HEK-293 Flp-In cells using GenElute mammalian total RNA purification kit (Sigma) according to the manufacturer's instructions, followed by DNase treatment (Invitrogen). cDNA was synthesized using a gene-specific primer for the pcDNA5/FRT vector (SMN1cDNA) and Superscript III reverse transcriptase (Invitrogen) according to the manufacturer's instructions. qRT-PCR analysis was performed using isoform-specific primers (Table S10) where each reaction contained 1 μL template cDNA, 10 pmol of

each primer, and 1X iQ SYBR green supermix (BioRAD) to a final volume of 25 µL. Reactions were carried out using a iCycler iQ system (BioRAD) for 30 cycles (95ºC for 15 s, 72ºC for 30 s). The purity of the PCR products was determined by melt curve analysis. Data analysis was completed using the iCycler IQ system software v.3.1.7050 (BioRAD). Isoform-specific relative expression was calculated using theΔCt (change in cycling threshold) (*S16*). Expression levels of duplicate PCR samples were normalized to the levels of *HPRT* (Hypoxanthine-guanine phosphoribosyltransferase**)**. Unless otherwise noted, data is reported as the ratio of the mean expression levels of the exon 7 excluded isoform to the exon 7 included isoform for the wild-type device relative to the same ratio for the mutant control device under the indicated ligand condition $\pm$ the average error.

**Statistical Analysis**

Data are expressed as relative expression (fold) or expression (fold) $\pm$ average error where applicable. Relative expression (fold) is taken to be: [(device response (+ligand))/(device response (-ligand))]/[(mutant device response (+ligand))/(mutant device response (-ligand))] or is the ratio of the expression of the wild-type device in the presence of ligand to the absence of ligand, normalized to the same ratio for the mutant RNA device. Expression (fold) is the ratio of the expression of the RNA device in the presence of ligand to the absence of ligand. Relative expression is the ratio of the expression of the wild-type device to the mutant device under the same condition. Student's *t*-test and Anova analyses were performed using Microsoft Excel. $P < 0.05$ were taken to be significant.

## Supporting Text

### Text S1: Data Reporting Methods and Controls

Gene expression can be sensitive to a myriad of external factors, such that appropriate controls are required to account for potential nonspecific effects of experimental procedures applied to cells. For example, gene expression activity measured through fluorescent reporters can be altered through nonspecific effects of the ligand on gene expression or cellular fluorescence through other cellular mechanisms. We conducted careful controls in the experiments reported in this study to ensure accurate accounting of any nonspecific effects of heterologous protein expression or exogenous ligand addition (when inducing pathway signaling) on gene expression and phenotypic responses (cell survival and death).

For each aptamer-containing device, a corresponding inactive sensor control (negative control) was constructed in which the wild-type aptamer was replaced by a mutated aptamer, such that the only difference between the device and its corresponding control was its ability to bind to its corresponding ligand. As such, measuring the difference in gene expression (or other measure of output activity) in the presence and absence of ligand for the negative control provides a measure of nonspecific effects of the ligand. The same measurement for the wild-type aptamer device provides a combined measure of specific and nonspecific effects of the ligand on the measured device output. To account for the non-aptamer-mediated effects of the ligand, we normalize the fold-change (ratio of signal in the presence and absence of ligand) of the wild-type device to that of the negative control. As it is assumed that the nonspecific effects of the ligand will be similar for a device containing a wild-type aptamer and its negative control, this value provides a measure of the specific effects of ligand binding to the sensor element on the gene

regulatory output of the device. The validity of such normalization methods for ligand-mediated gene-regulatory systems has been previously described (*S17*). We feel it is particularly useful in the systems used in this work as the addition of molecules that activate pathway signaling (i.e., TNF-α, $LTD_4$) may have significant nonspecific effects on cellular fluorescence, gene expression, or other cellular mechanisms.

The device responses are characterized through several different gene expression and phenotypic assays, and the reproducible agreement between these characterization methods provide further confirmation of their ligand-responsive gene-regulatory activities. Specifically, activity measurements based on transcript isoform (assayed through qRT-PCR) and fluorescent reporter levels (assayed through flow cytometry) generally agree with one another. In addition, for the majority of the devices the characterized device response is apparent in the unnormalized data for both fluorescent reporter and transcript isoform levels (Tables S1 to S6). The exception to this are for the devices that increase exon inclusion (MS2-6 and the NF-κB p50-responsive devices), where unnormalized gene expression data indicate no changes or slight increases in GFP levels in the presence of ligand. However, the fold change in GFP levels is significantly lower than all devices that increase exon exclusion, and the corresponding unnormalized transcript isoform levels support the reported device responses. The transcript isoform levels provide a more direct measure of splicing regulation from the devices, whereas cellular fluorescence is likely more influenced by any nonspecific effects of the ligands.

Finally, the ligand-specific responses of the devices are further supported by phenotypic assays that characterize cell survival and cell death within cell populations harboring individual devices in the presence and absence of appropriate ligands (Fig. 4). In a therapeutic application one would be more concerned with the absolute performance of the device. Therefore, we report

absolute measures of cell survival (or death) within a given cell population for the phenotypic assays and do not report values normalized to the relevant negative control. The negative controls are reported separately to demonstrate the specificity of ligand addition on the resulting phenotypic effect to cells harboring the functional devices. These assays demonstrate that the RNA devices are able to effectively regulate a phenotypic response in a manner that correlates with their characterized gene-regulatory activity. In addition, the data demonstrate that relatively moderate gene-regulatory effects (~2-4-fold) can be used to effectively regulate downstream functional outputs when linked to potent upstream regulators. This observation is supported by other recent work on engineered RNA regulatory systems applied to the regulation of T-cell proliferation (*S17*) and bacterial chemotaxis (*S18*).

**Text S2: Mechanisms by which Protein Binding can Alter Splicing Patterns**

Previous experiments have shown that the binding of antisense oligonucleotides to a transcript can either enhance or inhibit the inclusion of an alternatively spliced exon depending on the location of binding within the transcript (*S19*). These studies have shown that oligonucleotide binding to the transcript can block key cis-acting signals that act to recruit enhancers, silencers, or spliceosomal components. Other experiments have shown that bifunctional antisense oligonucleotides, which harbor an antisense region and a binding sequence for a splicing factor, can be used to recruit splicing factors to specific transcript locations (*S3, S20*). Different effects on alternative splicing (i.e., exclusion or inclusion) have been observed, depending on the identity of the recruited splicing factors (*S21, S22*).

These earlier studies support that the recruitment of proteins to a transcript through

binding to an integrated aptamer sequence can alter splicing patterns through two different mechanisms. First, the recruited protein can hinder the binding of other trans-acting splicing factors or spliceosomal components. For example, by hindering the binding of enhancers or spliceosomal components protein binding would result in increased exon exclusion, whereas by hindering the binding of silencers it would result in increased inclusion. Second, the recruited protein may in turn act to recruit other splicing factors to the transcript through protein-protein interactions between the protein ligand and the splicing factor. The resulting splicing pattern would depend on whether an enhancer or silencer was recruited to the transcript. Therefore, the resulting effect of protein binding to the aptamer would be a function of the relative location in the transcript (i.e., aptamer location relative to other cis-acting splicing regulatory sequences) and the identity of the protein (i.e., any protein-protein interaction domains that would allow the protein to recruit other factors that would in turn affect splicing).

The results described here can be explained in the context of this mechanistic model. Position-dependent effects of aptamer integration can be explained by the relative distances of the sites from cis-acting splicing sequences, where positions 3, 6, and 10 are located at critical distances from the 5’ splice site, the branch point, and the 3’ splice site. In addition, the different effects on alternative splicing observed from different protein ligands at identical aptamer integration positions (e.g., p50 and p65) can be explained by protein-specific and ligand binding properties. For example, p65 may result in increased exon exclusion through steric hindrance of an enhancer or spliceosomal component, whereas p50 may result in increased exon inclusion by interacting with and recruiting a splicing factor that acts to enhance splicing. The two proteins have contrasting structural domains that mediate protein-protein interactions, where p65 has a trans-activation domain and p50 has a trans-repression domain (*S23*). In addition, the affinities of

both aptamers for their cognate ligand differ by 2-fold (*S8*, *S24*), and the overall conformation and size of the protein dimers bound to the RNA aptamers are different.

Based on this mechanism, we would not expect a small molecule aptamer to control alternative splicing in the described platform. Unlike many other synthetic riboswitch platforms, the described system does not function through a conformational switching event or stabilization of a particular secondary structure through ligand binding, which are mechanisms amenable to control through small molecule ligand binding. The described system functions through the recruitment of a protein ligand to the transcript, which can them sterically hinder the assembly of other trans-acting splicing factors or spliceosomal components or aid in the recruitment of these factors. Small molecule ligands would not be able to act through these mechanisms.

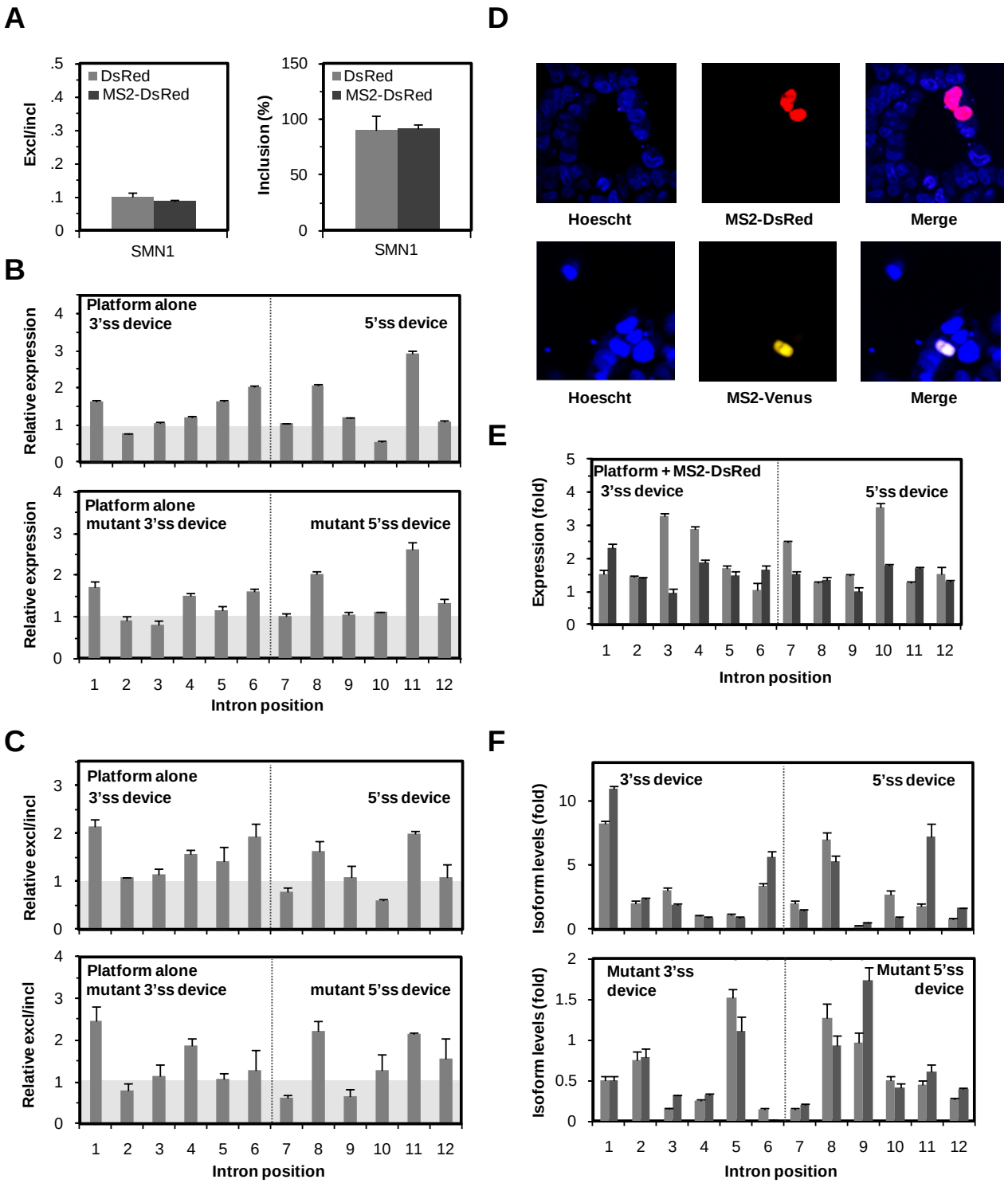


**Figure S1. Additional expression and transcript isoform analysis of the MS-responsive devices and nuclear localization of MS2-DsRed/MS2-Venus**

(A) Transcript isoform analysis of the SMN1-GFP construct (which harbors a natural stop codon in the alternatively spliced exon) lacking an aptamer input module with primer sets specific for exon 7 excluded and included products demonstrates that the presence of the MS2-DsRed fusion protein does not alter splicing patterns. For all qRT-PCR data, expression levels of duplicate samples were normalized to the levels of *HPRT*. Data is reported as the ratio of the mean expression levels of the exon 7 excluded isoform to the exon 7 included isoform $\pm$ the average error. Exon inclusion percentages are shown. All error bars represent +/- s.d. from the mean values determined from two independent experiments. (B) The integration of the wild-type and mutant aptamer input modules can affect the regulatory output of the device. The observed effects are consistent between those observed from the wild-type (upper panel) and mutant (lower panel) aptamer input modules in the absence of ligand. Activities are reported as relative expression by taking the ratio of the mean GFP levels of the indicated RNA device to that from the SMN1-GFP construct lacking an aptamer input module as determined from flow cytometry analysis. For all reported activities, expression levels were determined by flow cytometry analysis from two independent experiments. (C) Transcript isoform analysis of the wild-type (upper panel) and mutant (lower panel) MS2-responsive devices. qRT-PCR data supports gene expression data (Fig. S1B). Data is reported as the ratio of the mean expression levels of the exon 7 excluded isoform to the exon 7 included isoform for the wild-type and mutant devices relative to the same ratio for the SMN1-GFP construct lacking an aptamer input module. (D) Confocal images of HEK293 Flp-In cells expressing the MS2-DsRed and MS2-Venus fusion constructs. The MS2-DsRed and MS2-Venus fusion proteins colocalize with the Hoescht nuclear stain in cells transiently expressing the constructs. (E) The response of the MS2-responsive device to heterologously expressed MS2-DsRed fusion protein is affected by the location of the input module and demonstrates specificity of device response to the wild-type aptamer. Activities for the wild-type (light gray bars) and mutant devices (dark gray bars) are reported as expression (fold), where the ratio of the mean GFP level of the device in the presence of MS2-DsRed (presence of ligand) is normalized to the mean GFP level in the presence of DsRed alone (absence of ligand). (F) Transcript isoform analysis of the wild-type (upper panel) and mutant (lower panel) MS2-responsive devices with primer sets specific for exon 7 excluded (light gray bars) and included (dark gray bars) products. Transcript isoform levels are reported as isoform levels (fold), where the mean isoform level in the presence of MS2-DsRed (presence of ligand) is normalized to the mean isoform level in the presence of DsRed alone (absence of ligand) $\pm$ the average error.

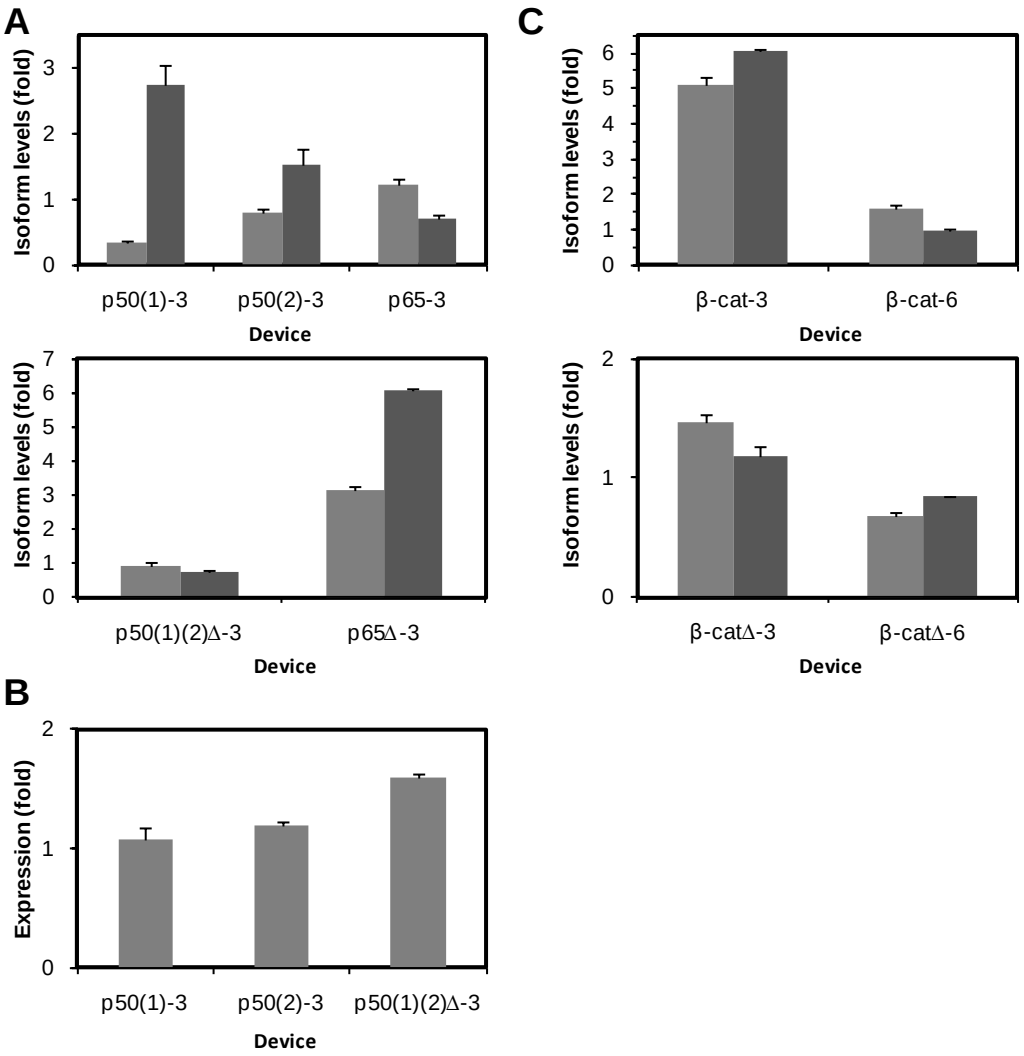


**Figure S2. Transcript isoform and expression analysis of the NF-κB- and β-catenin-responsive devices**

(A) Transcript isoform analysis of the wild-type (upper panel) and mutant (lower panel) NF-κB-responsive devices with primer sets specific for exon 7 excluded (light gray bars) and included (dark gray bars) products. Transcript isoform levels are reported as isoform levels (fold), where the mean isoform level in the presence of TNF-α (presence of ligand) is normalized to the mean isoform level in the presence of water alone (absence of ligand) $\pm$ the average error. (B) The NF-κB p50-responsive devices exhibit responses to a heterologously expressed p50-DsRed fusion protein similar to that observed with TNF-α stimulation. Activities for the wild-type and mutant NF-κB p50-responsive devices are reported as expression (fold), where the mean GFP level of the device in the presence of p50-DsRed (presence of ligand) is normalized to the mean GFP level in the presence of DsRed alone (absence of ligand). (C) Transcript isoform analysis of the wild-type (upper panel) and mutant (lower panel) β-catenin-responsive devices with primer sets specific for exon 7 excluded (light gray bars) and included (dark gray bars) products. Transcript isoform levels are reported as isoform levels (fold), where the mean isoform level in the presence of $LTD_4$ (presence of ligand) is normalized to the mean isoform level in the presence of water alone (absence of ligand) $\pm$ the average error.

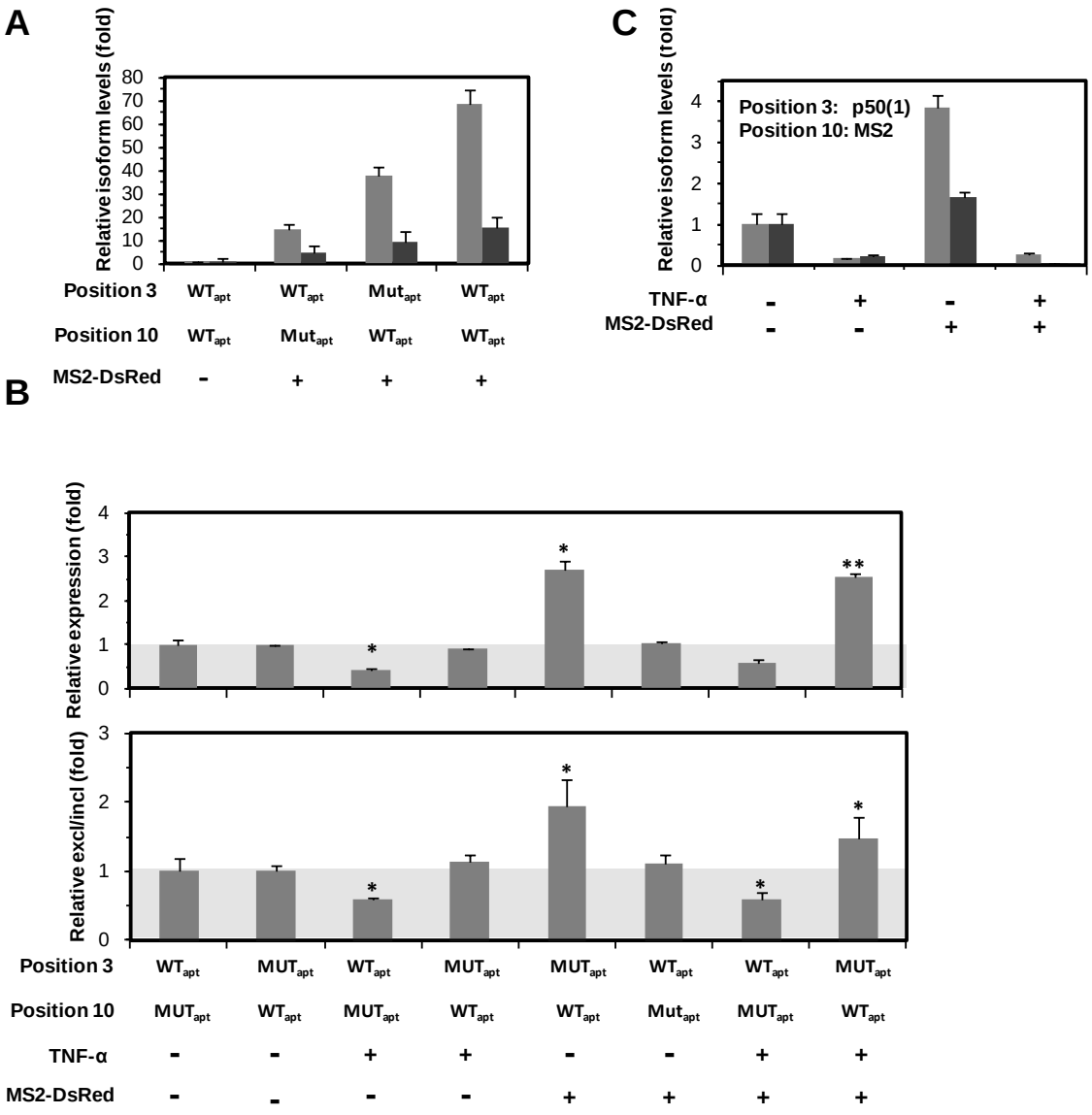


**Figure S3. Transcript isoform analysis of the multi-input processing RNA devices and control responses**

(A) Transcript isoform analysis of the MS2 multi-input processing regulatory devices with primer sets specific for exon 7 excluded (light gray bars) and included (dark gray bars) products. Relative isoform levels (fold) are reported by dividing the mean isoform level in the presence of MS2-DsRed (presence of ligand) by the mean isoform level observed with DsRed alone (absence of ligand) $\pm$ the average error, where this ratio is normalized by the corresponding ratio for the double mutant control device. Transcript isoform analysis of the MS2 multi-input processing devices also supports gene expression data. (B) The MS2 / NF-κB p50 multi-input processing device response is specific for the MS2 and NF-κB p50 ligands. Combinations of the NF-κB p50

and MS2 aptamers (wild-type and mutant) were inserted into positions 3 and 10, respectively. *P*-values derived from the Student's t-test for all reported activities are as follows: $*P < 0.05$ and $**P < 0.01$. Relative expression (fold) and relative excl/incl (fold) were determined as described in Fig. 1E. (C) Transcript isoform analysis of the MS2 / NF-κB p50 multi-input processing devices with primer sets specific for exon 7 excluded (light gray bars) and included (dark gray bars) products.

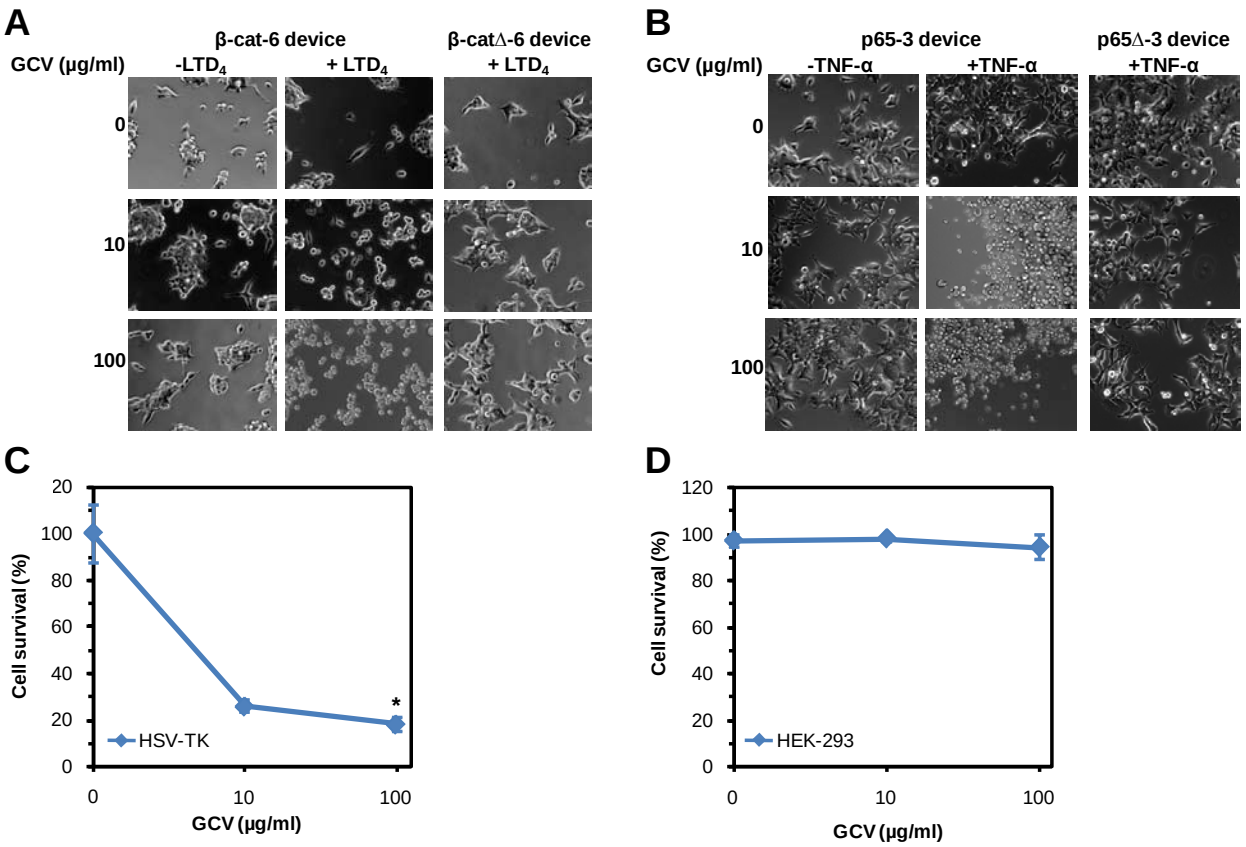


**Figure S4. Analysis of cell survival in wild-type and stable cell lines expressing HSV-TK output module devices**

(A, B) Phase images of the β-catenin- (A) and NF-κB-responsive (B) devices fused to *HSV-TK*. Increased cell death from the β-catenin- and NF-κB-responsive devices is specific to pathway stimulation, GCV, and the wild-type aptamers. (C) Dose-response curve of cell survival percentages for HEK-293 cells stably expressing HSV-TK from a CMV promoter. Survival percentages of cells exposed to GCV (0-100 μg/ml) were assessed by flow cytometry. (D) Dose-response curve of cell survival percentages for wild-type HEK-293 cells. Survival percentages of cells exposed to GCV (0-100 μg/ml) were assessed by flow cytometry. *P*-values derived from the Student's t-test for all reported activities are as follows: $*P < 0.05$ and $**P < 0.01$.

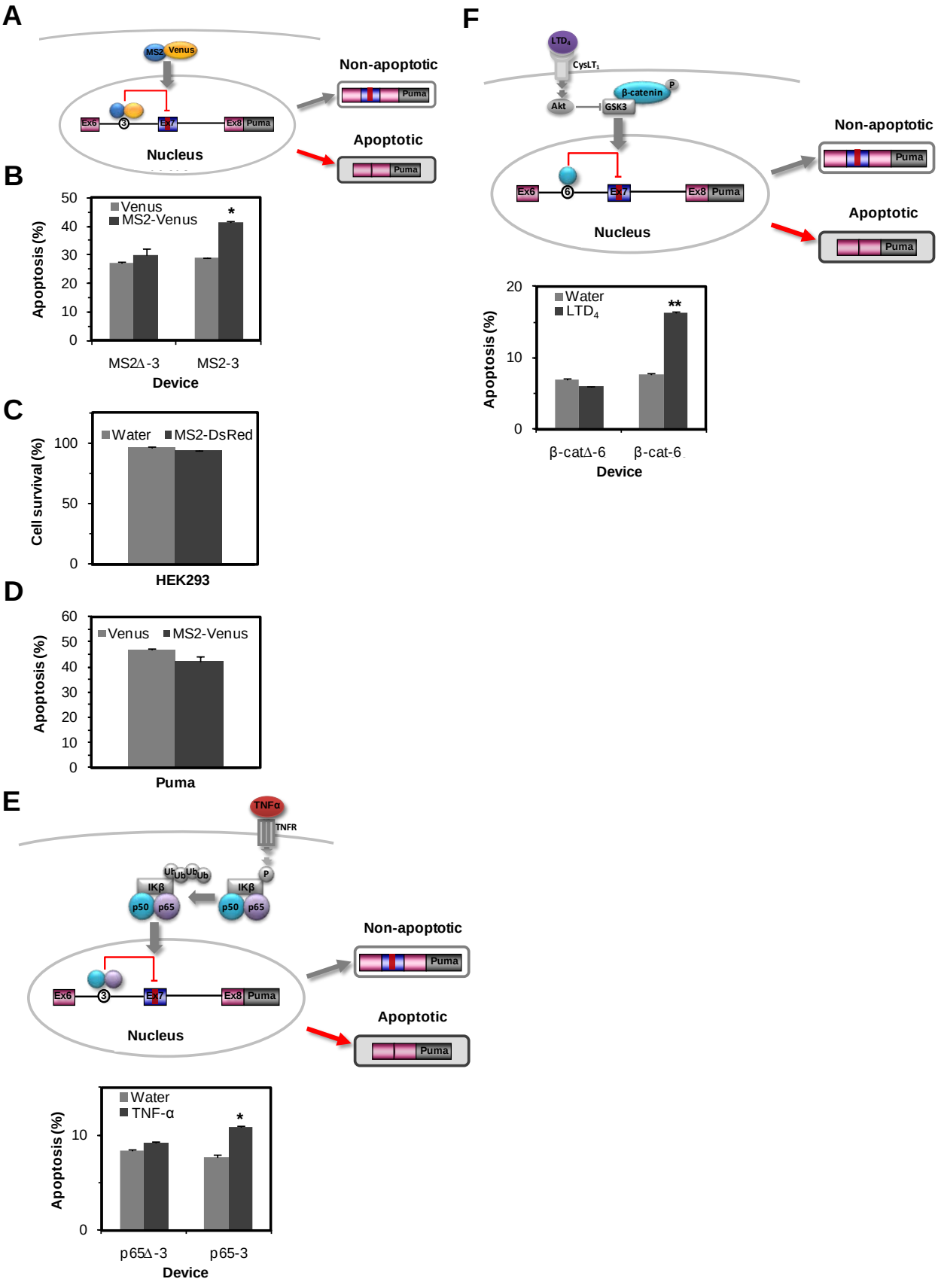
A
MS2
Venus
Non-apoptotic
Puma
Ex6
3
Ex7
Ex8
Puma
Nucleus
Apoptotic
Puma
B
Venus
MS2-Venus
*
Apoptosis (%)
50
40
30
20
10
0
MS2Δ-3
MS2-3
Device
C
Water
MS2-DsRed
Cell survival (%)
100
50
0
HEK293
D
Venus
MS2-Venus
Apoptosis (%)
60
50
40
30
20
10
0
Puma
E
TNFα
TNFR
P
Ub
IKβ
p50
p65
Non-apoptotic
Puma
Ex6
3
Ex7
Ex8
Puma
Nucleus
Apoptotic
Puma
Water
TNF-α
*
Apoptosis (%)
10
0
p65Δ-3
p65-3
Device
F
LTD4
CysLT1
β-catenin
P
Akt
GSK3
Non-apoptotic
Puma
Ex6
6
Ex7
Ex8
Puma
Nucleus
Apoptotic
Puma
Water
LTD4
**
Apoptosis (%)
20
10
0
β-catΔ-6
β-cat-6
Device

**Figure S5. Analysis of cell survival/apoptosis percentages in transiently transfected HEK293 cells and stable cell lines expressing Puma output module devices**

We replaced the *GFP* coding sequence with the proapoptotic gene *Puma*, where the overexpression of Puma induces rapid apoptosis (*S25*). (A) Mechanism of the MS2-responsive device fused to an output module that results in apoptosis (*Puma*). (B) The MS2-responsive (MS2-3) device fused to *Puma* triggers increased levels of apoptosis in cells heterologously expressing the MS2-Venus fusion protein. Apoptosis of the wild-type and mutant devices was assessed by flow cytometry (as described in Materials and Methods) in the presence of the MS2-Venus fusion and Venus. For all reported activities, the mean cell survival and apoptosis levels from two independent experiments are shown. Cells stably expressing the MS2 device (MS2-3) linked to *Puma* displayed a 50% increase in apoptosis in the presence of a MS2-Venus (fluorescent protein) fusion construct compared to cells transfected with Venus alone, whereas the mutant MS2 device resulted in an insignificant response (~10%). (C) Flow cytometry analysis of cell survival percentages of HEK293 cells alone and in the presence of MS2-DsRed. The results demonstrate that HEK293 cells have a high level of cell viability that is not affected by transient transfection. (D) Flow cytometry analysis of apoptosis in HEK293 cells stably expressing Puma alone. Apoptosis of this cell line was assessed in the presence of the MS2-Venus fusion and Venus alone. (E, F) Mechanisms of the β-catenin- and NF-κB-responsive devices fused to the apoptosis output module (*Puma*), which trigger apoptosis in response to detection of disease markers. The β-catenin- (β-cat-6) and NF-κB p65-responsive (p65-3) devices fused to *Puma* trigger increased levels of apoptosis in cells where signaling has been stimulated through these pathways. Stimulation of the β-catenin pathway led to a significant ~2-fold increase in apoptosis in cells stably expressing the β-cat-6 device ($P < 0.01$). Cells stably expressing the p65-3 devices exhibited a 40% increase in apoptosis in response to TNF-α ($P < 0.05$). Apoptosis was assessed by flow cytometry in the presence and absence of the appropriate stimulation molecule (TNF-α or $LTD_4$).

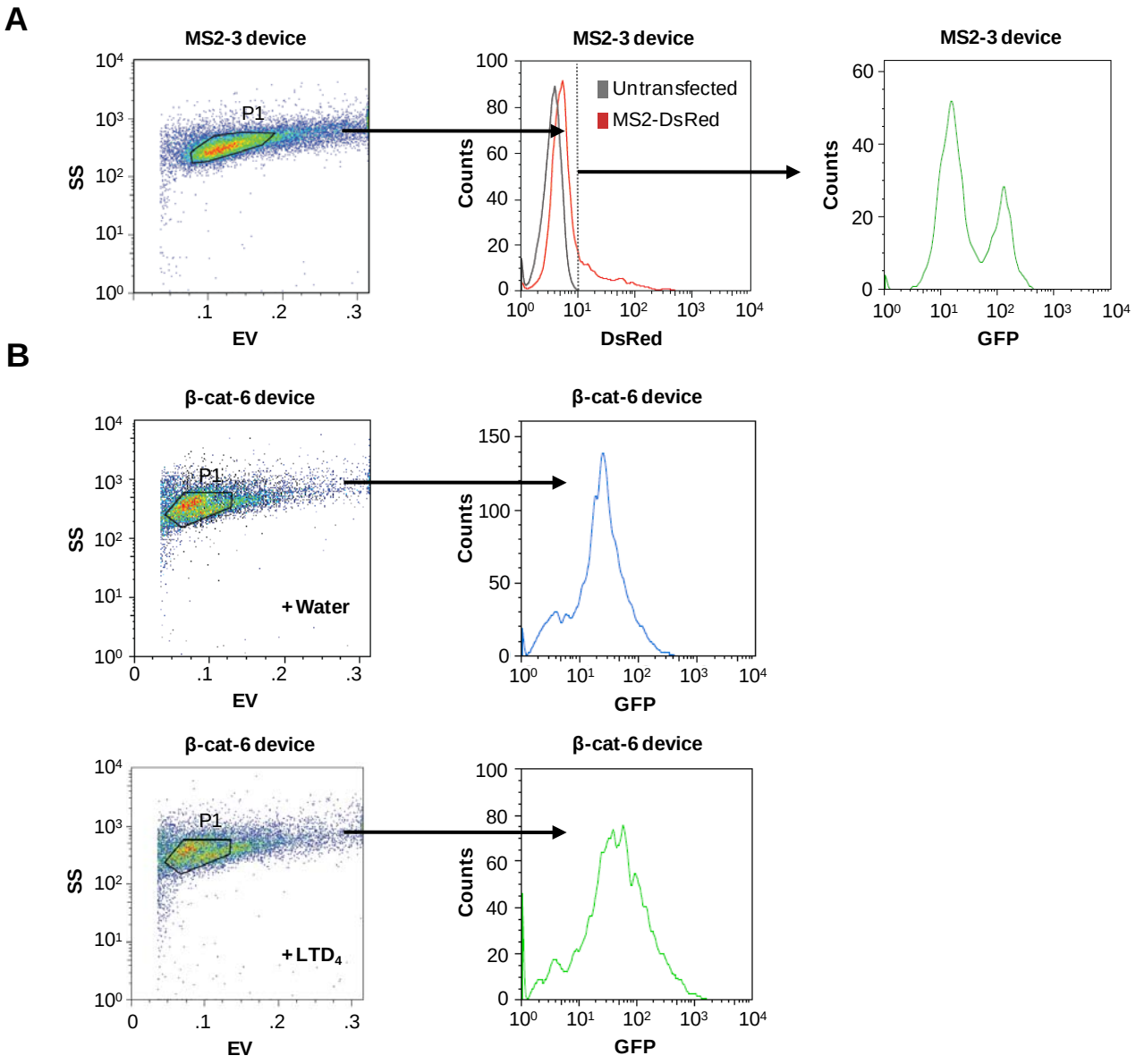


**Figure S6. Flow cytometry analysis and gating procedures for the MS2- and β-catenin-responsive devices**

(A) Flow cytometry and gating procedure for all MS2-responsive devices. As an example, flow cytometry data from the MS2-3 device is presented. Dot plots show initial gating of viable stable cells (P1), followed by gating for all MS2-DsRed positive cells. The histogram reports the intensity of GFP fluorescence in the MS2-DsRed population. (B) Flow cytometry and gating procedure for all β-catenin-responsive devices. As an example, flow cytometry data from the β-cat-6 device is presented. Dot plots show initial gating of viable stable cells (P1) in the presence of water or the $LTD_4$ inducer. The resulting histogram reports the intensity of GFP fluorescence in the viable cell population. An identical gating procedure was followed for the flow cytometry analysis of the NF-κB-responsive devices.

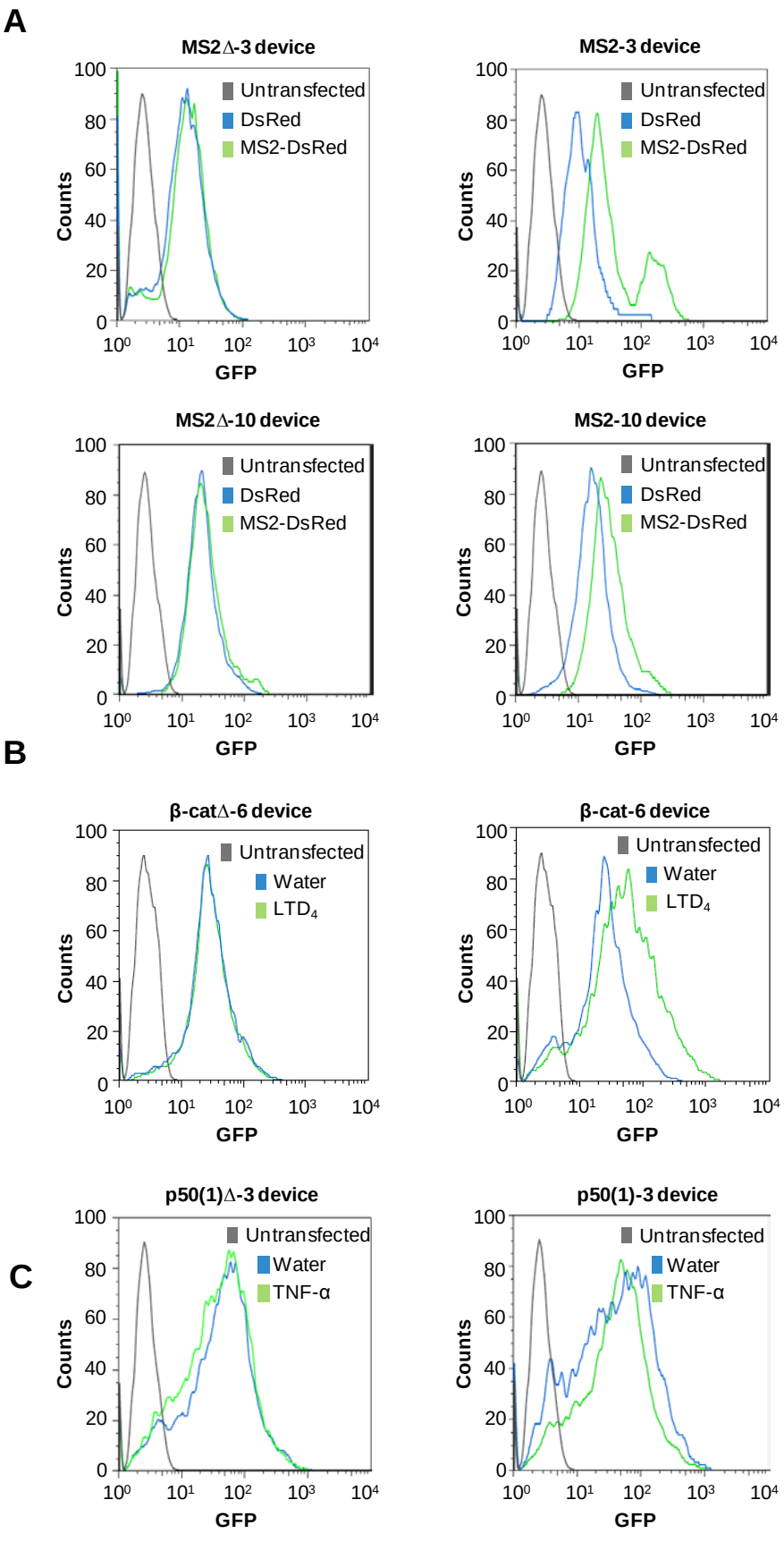
A
MS2Δ-3 device
MS2-3 device
MS2Δ-10 device
MS2-10 device
Untransfected
DsRed
MS2-DsRed
Counts
GFP
B
β-catΔ-6 device
β-cat-6 device
Water
LTD4
C
p50(1)Δ-3 device
p50(1)-3 device
TNF-α

**Figure S7. Representative flow cytometry histograms for the MS2-, β-catenin- and NF-κB-responsive devices**

(A) Representative flow cytometry histograms for the MS2-responsive devices. The histograms report the intensity of GFP fluorescence for both the wild-type and mutant MS2-3 and MS2-10 regulatory devices in the presence of DsRed and MS2-DsRed. The mutant devices show a minimal change in GFP fluorescence in the presence of MS2-DsRed, while wild-type devices show a significant change in response to MS2-DsRed. The fluorescence data shown here is presented in Fig. 1E (B) Representative flow cytometry histograms for the β-catenin-responsive devices. The histograms report the intensity of GFP fluorescence for both the wild-type and mutant β-cat-6 regulatory devices in the presence of water or $LTD_4$. The mutant device shows a minimal change in GFP fluorescence in the presence of $LTD_4$, while the wild-type device shows a significant increase in fluorescence in response to $LTD_4$. The fluorescence data shown here is presented in Fig. 2F (C) Representative flow cytometry histograms for the NF-κB-responsive devices. The histograms report the intensity of GFP fluorescence for both the wild-type and mutant p50(1)-3 regulatory devices in the presence of water or TNF-α. The mutant device shows a minimal change in GFP fluorescence in the presence of TNF-α, while the wild-type device shows a significant decrease in fluorescence in response to TNF-α. The fluorescence data shown here is presented in Fig. 2C.

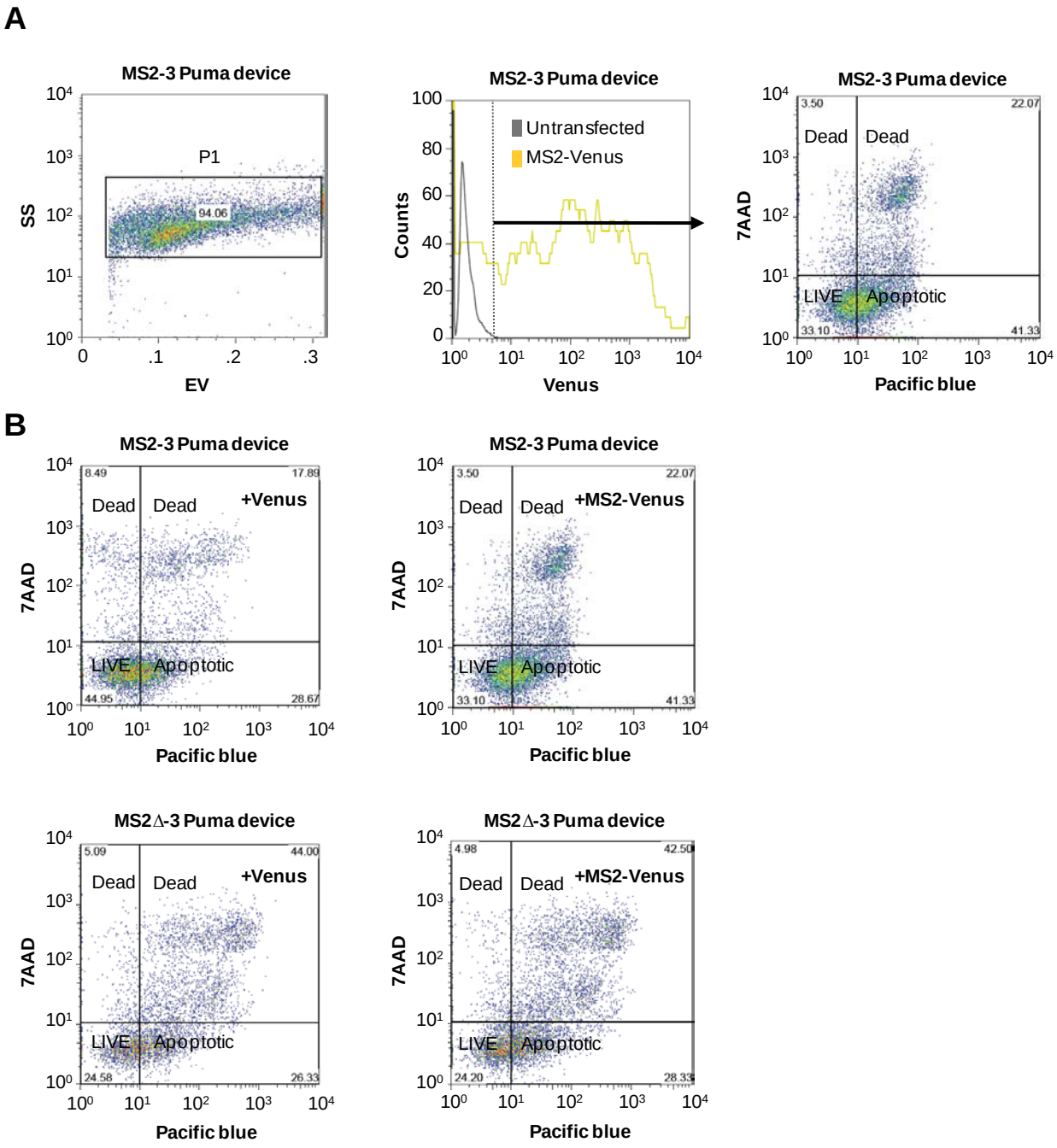


**Figure S8. Representative flow cytometry gating procedures and histograms for the MS2-3-Puma apoptosis studies**

(A) Flow cytometry and gating procedure for the MS2-3-Puma device mediated apoptosis. Cells were stained with Pacific blue annexin V and 7AAD using the Vybrant Apoptosis Assay Kit (Invitrogen) according to the manufacturer's instructions. The positioning of all gates are based on the individual gates established for each single color control and can vary slightly between experiments. Dot plots show initial gating of all stable cells (P1), followed by gating for all MS2-

Venus positive cells. The final gated dot plot reports on the stages of programmed cell death for each cell line using a dual parameter staining consisting of Pacific blue annexin V and 7AAD. Briefly, live cells are Pacific blue annexin V negative and 7AAD negative, apoptotic cells are Pacific blue annexin V positive and 7AAD negative, and dead cells are 7AAD positive. (B) Flow cytometry analysis of the MS2-3-Puma devices. The dot plots report on the stages of programmed cell death for both the wild-type and mutant MS2-3-Puma regulatory devices in the presence of Venus or MS2-Venus. The percentage of apoptotic cells shown here are reported in Fig. S5B.

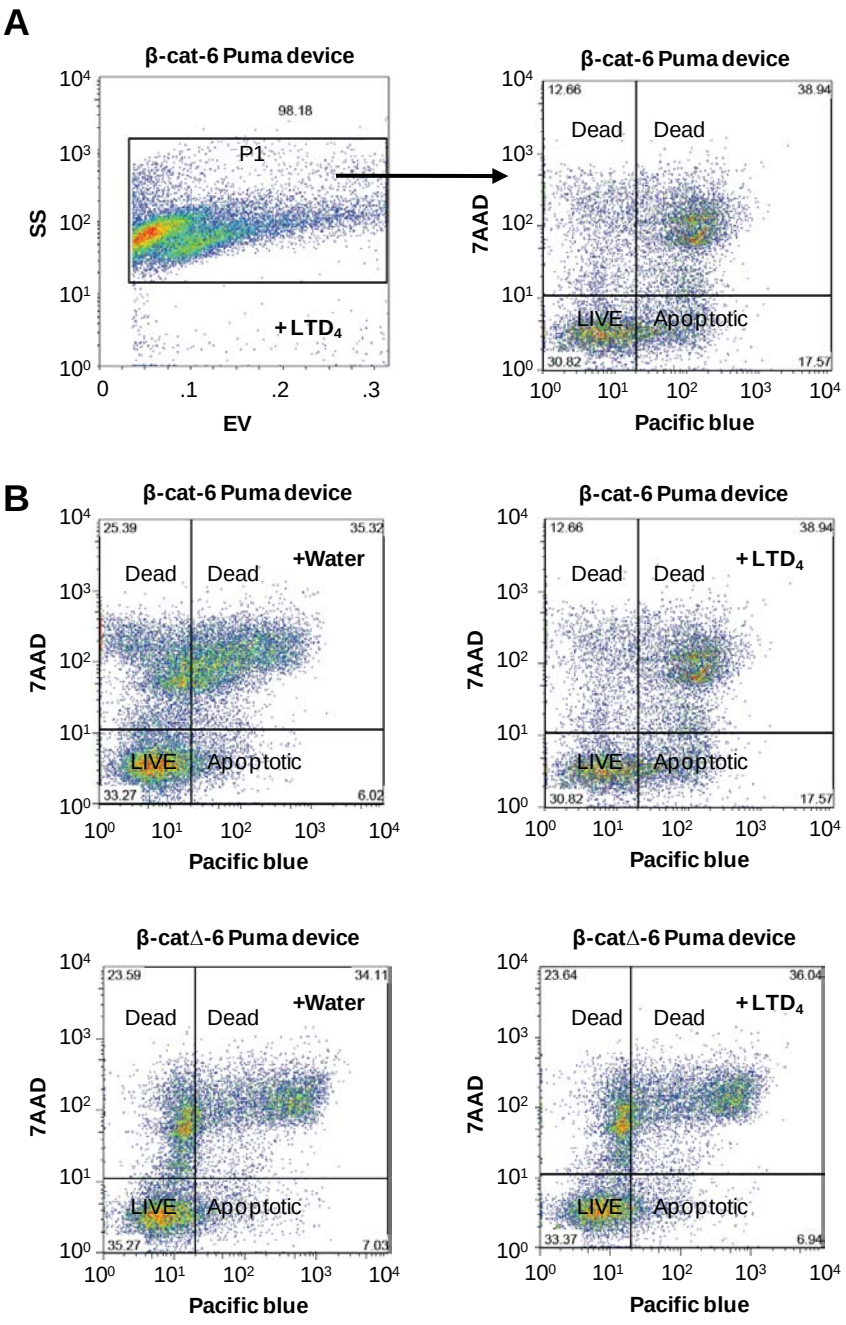


**Figure S9. Representative flow cytometry gating procedures and histograms for the β-cat-6-Puma apoptosis studies**

(A) Flow cytometry and gating procedure for the β-cat-6-Puma device mediated apoptosis. Cells were stained with Pacific blue annexin V and 7AAD. Dot plots show initial gating of all stable cells (P1) and the resulting gated dot plot reports on the stage of programmed cell death for each cell line. (B) Flow cytometry analysis of the β-cat-6-Puma devices. The dot plots report on the stages of programmed cell death for both the wild-type and mutant β-cat-6-Puma regulatory

devices in the presence of water or $LTD_4$. The percentage of apoptotic cells shown here are reported in Fig. S5F. The gating procedure shown in panel (A) was followed for the flow cytometry analysis of the NF-κB-Puma regulatory devices.

| Aptamer | MS2 | | | | | | MS2Δ | | | | | |
|---|---|---|---|---|---|---|---|---|---|---|---|---|
| Protein | DsRed | | MS2-DsRed | | Expression | Excl/incl | DsRed | | MS2-DsRed | | Expression | Excl/incl |
| Position | Avg. RFU | Stdev. | Avg. RFU | Stdev. | (fold) | (fold) | Avg. RFU | Stdev. | Avg. RFU | Stdev. | (fold) | (fold) |
| 1 | 13.42 | 0.01 | 20.47 | 2.98 | 1.53 | 0.76 | 11.73 | 1.51 | 27.34 | 0.04 | 2.33 | 1.00 |
| 2 | 11.74 | 0.16 | 17.19 | 0.18 | 1.46 | 0.90 | 7.19 | 0.23 | 10.21 | 0.01 | 1.42 | 0.97 |
| 3 | 20.72 | 0.81 | 68.35 | 5.45 | 3.30 | 1.57 | 21.01 | 2.80 | 20.02 | 0.42 | 0.95 | 0.50 |
| 4 | 21.84 | 0.63 | 63.19 | 5.17 | 2.89 | 1.19 | 24.33 | 0.47 | 45.44 | 3.59 | 1.87 | 0.81 |
| 5 | 19.58 | 1.66 | 33.44 | 1.35 | 1.71 | 1.19 | 15.65 | 0.16 | 23.46 | 2.46 | 1.50 | 1.37 |
| 6 | 23.46 | 2.46 | 24.21 | 0.25 | 1.03 | 0.59 | 24.12 | 5.42 | 39.83 | 1.77 | 1.65 | 5.66 |
| 7 | 29.77 | 0.53 | 74.42 | 2.88 | 2.50 | 1.41 | 14.49 | 0.48 | 21.96 | 2.43 | 1.52 | 0.73 |
| 8 | 11.62 | 0.11 | 14.82 | 0.28 | 1.28 | 1.32 | 14.07 | 0.99 | 18.83 | 1.03 | 1.34 | 1.37 |
| 9 | 8.39 | 0.23 | 12.61 | 0.28 | 1.50 | 0.62 | 13.90 | 1.46 | 14.05 | 0.33 | 1.01 | 0.55 |
| 10 | 2.96 | 0.37 | 10.44 | 0.30 | 3.53 | 3.03 | 13.22 | 0.14 | 23.62 | 1.52 | 1.79 | 1.19 |
| 11 | 24.04 | 0.23 | 30.60 | 1.63 | 1.27 | 0.25 | 18.92 | 0.81 | 32.10 | 0.04 | 1.70 | 0.73 |
| 12 | 34.72 | 3.91 | 53.80 | 9.44 | 1.55 | 0.50 | 18.84 | 0.47 | 24.47 | 0.35 | 1.30 | 0.68 |

**Table S1.** Raw data from flow cytometry and transcript isoform analysis and for the MS2-responsive devices (Fig. 1E). For each device, the average relative fluorescence units (RFU) is shown along with the standard deviation (Stdev) between each duplicate sample. For each device the fold change in GFP expression (Expression (fold)) and the fold change in the ratio of exon 7 excluded isoform levels to exon 7 included isoform levels (Excl/incl (fold)) (as determined by qRT-PCR analysis; Fig. 1E and Fig. S1F) in the presence and absence of ligand are shown.

| **Time (h)** | 0 | | | | | 6 | | | | | 12 | | | | |
|---|---|---|---|---|---|---|---|---|---|---|---|---|---|---|---|
| **Stimuli** | Water | | TNF-α | | **Expression** | Water | | TNF-α | | **Expression** | Water | | TNF-α | | **Expression** |
| **Device** | **Avg. RFU** | **Stdev.** | **Avg. RFU** | **Stdev.** | **(fold)** | **Avg. RFU** | **Stdev.** | **Avg. RFU** | **Stdev.** | **(fold)** | **Avg. RFU** | **Stdev.** | **Avg. RFU** | **Stdev.** | **(fold)** |
| p50(1)-3 | 66.59 | 3.48 | 66.43 | 3.88 | 1.00 | 79.49 | 0.00 | 74.59 | 1.53 | 0.94 | 85.74 | 4.38 | 78.45 | 0.78 | 0.91 |
| p50(1)(2)Δ-3 | 64.13 | 1.00 | 64.12 | 0.90 | 1.00 | 77.29 | 1.15 | 75.09 | 1.33 | 0.97 | 83.29 | 1.82 | 102.49 | 1.99 | 1.23 |
| p50(2)-3 | 30.70 | 2.27 | 30.35 | 0.28 | 0.99 | 33.43 | 1.50 | 31.55 | 0.10 | 0.94 | 34.62 | 0.59 | 34.20 | 1.34 | 0.99 |
| p65-3 | 54.26 | 0.62 | 51.72 | 0.89 | 0.95 | 56.03 | 1.56 | 52.39 | 1.13 | 0.94 | 69.82 | 5.56 | 76.70 | 2.09 | 1.10 |
| p65Δ-3 | 35.25 | 0.30 | 35.03 | 0.42 | 0.99 | 37.68 | 1.72 | 35.10 | 1.29 | 0.93 | 47.21 | 4.75 | 44.45 | 1.20 | 0.94 |

| **Time (h)** | 24 | | | | | 36 | | | | | 48 | | | | | |
|---|---|---|---|---|---|---|---|---|---|---|---|---|---|---|---|---|
| **Stimuli** | Water | | TNF-α | | **Expression** | Water | | TNF-α | | **Expression** | Water | | TNF-α | | **Expression** | **Excl/incl** |
| **Device** | **Avg. RFU** | **Stdev.** | **Avg. RFU** | **Stdev.** | **(fold)** | **Avg. RFU** | **Stdev.** | **Avg. RFU** | **Stdev.** | **(fold)** | **Avg. RFU** | **Stdev.** | **Avg. RFU** | **Stdev.** | **(fold)** | **(fold)** |
| p50(1)-3 | 93.51 | 0.00 | 66.83 | 0.49 | 0.71 | 86.88 | 1.34 | 78.88 | 1.20 | 0.91 | 78.45 | 0.00 | 73.85 | 0.26 | 0.94 | 0.12 |
| p50(1)(2)Δ-3 | 90.70 | 0.54 | 98.99 | 1.61 | 1.09 | 102.36 | 7.70 | 117.84 | 1.66 | 1.15 | 77.52 | 1.50 | 124.40 | 3.00 | 1.60 | 1.27 |
| p50(2)-3 | 31.13 | 0.42 | 26.52 | 2.06 | 0.85 | 28.82 | 1.30 | 16.76 | 1.43 | 0.58 | 30.14 | 0.80 | 25.74 | 2.09 | 0.85 | 0.54 |
| p65-3 | 64.52 | 1.57 | 76.34 | 2.53 | 1.18 | 61.90 | 3.11 | 86.23 | 0.12 | 1.39 | 54.96 | 1.51 | 104.31 | 3.30 | 1.90 | 1.74 |
| p65Δ-3 | 41.34 | 1.01 | 38.39 | 1.02 | 0.93 | 34.75 | 1.97 | 33.36 | 0.60 | 0.96 | 36.79 | 1.67 | 30.97 | 0.61 | 0.84 | 0.52 |

**Table S2.** Raw data from flow cytometry analysis for the NF-κB-responsive devices (Fig. 2C). The same mutant device (p50(1)(2)Δ -3) was used for the normalization of the NF-κB p50 device data. For each device, the average relative fluorescence units (RFU) is shown along with the standard deviation (Stdev) between each duplicate sample. For each device the fold change in GFP expression and the fold change in the ratio of exon 7 excluded isoform levels to exon 7 included isoform levels (Excl/incl) (as determined by qRT-PCR analysis at 48 h; Fig. 2C and Fig. S2A) in the presence and absence of ligand are shown.

| Aptamer | p50 | | | | | p50Δ | | | | |
|---|---|---|---|---|---|---|---|---|---|---|
| Protein | DsRed | | p50-DsRed | | Expression | DsRed | | MS2-DsRed | | Expression |
| Device | Avg. RFU | Stdev. | Avg. RFU | (fold) | (fold) | Avg. RFU | Stdev. | Avg. RFU | Stdev. | (fold) |
| p50(1)-3 | 26.85 | 1.31 | 28.94 | 2.43 | 1.08 | 32.40 | 1.15 | 51.81 | 0.34 | 1.60 |
| p50(2)-3 | 18.63 | 0.57 | 22.12 | 0.36 | 1.19 | | | | | |

**Table S3.** Raw data from flow cytometry analysis for the p50-NF-κB-responsive devices (Fig. 2D). The same mutant device (p50(1)(2)Δ-3) was used for the normalization of the NF-κB p50 device data. For each device, the average relative fluorescence units (RFU) is shown along with the standard deviation (Stdev) between each duplicate sample. For each device the fold change in GFP expression in the presence and absence of ligand is shown.

| **Time (h)** | 0 | | | | | 6 | | | | | 12 | | | | |
|---|---|---|---|---|---|---|---|---|---|---|---|---|---|---|---|
| **Stimuli** | Water | | $LTD_4$ | | **Expression** | Water | | $LTD_4$ | | **Expression** | Water | | $LTD_4$ | | **Expression** |
| **Device** | **Avg. RFU** | **Stdev.** | **Avg. RFU** | **Stdev.** | **(fold)** | **Avg. RFU** | **Stdev.** | **Avg. RFU** | **Stdev.** | **(fold)** | **Avg. RFU** | **Stdev.** | **Avg. RFU** | **Stdev.** | **(fold)** |
| β-cat-3 | 39.23 | 2.21 | 37.85 | 0.76 | 0.96 | 39.87 | 2.16 | 37.31 | 0.78 | 0.94 | 43.00 | 0.68 | 41.14 | 1.22 | 0.96 |
| β-catΔ-3 | 62.41 | 4.53 | 54.60 | 5.46 | 0.87 | 63.42 | 1.39 | 73.50 | 0.05 | 1.16 | 67.42 | 1.30 | 65.93 | 2.86 | 0.98 |
| β-cat-6 | 78.74 | 1.46 | 80.19 | 0.93 | 1.02 | 86.25 | 0.18 | 82.12 | 0.46 | 0.95 | 86.51 | 1.20 | 95.23 | 2.91 | 1.10 |
| β-catΔ-6 | 64.90 | 0.37 | 63.58 | 5.88 | 0.98 | 67.35 | 1.80 | 70.86 | 1.61 | 1.05 | 69.14 | 1.39 | 69.91 | 1.51 | 1.01 |

| **Time (h)** | 24 | | | | | 36 | | | | | 48 | | | | | |
|---|---|---|---|---|---|---|---|---|---|---|---|---|---|---|---|---|
| **Stimuli** | Water | | $LTD_4$ | | **Expression** | Water | | $LTD_4$ | | **Expression** | Water | | $LTD_4$ | | **Expression** | **Excl/incl** |
| **Device** | **Avg. RFU** | **Stdev.** | **Avg. RFU** | **Stdev.** | **(fold)** | **Avg. RFU** | **Stdev.** | **Avg. RFU** | **Stdev.** | **(fold)** | **Avg. RFU** | **Stdev.** | **Avg. RFU** | **Stdev.** | **(fold)** | **(fold)** |
| β-cat-3 | 44.72 | 0.42 | 41.76 | 0.72 | 0.93 | 41.76 | 1.24 | 37.74 | 0.47 | 0.90 | 35.66 | 1.51 | 36.05 | 0.49 | 1.01 | 0.84 |
| β-catΔ-3 | 69.22 | 2.72 | 65.42 | 2.01 | 0.95 | 60.04 | 4.21 | 56.98 | 1.63 | 0.95 | 47.75 | 0.21 | 51.95 | 0.91 | 1.09 | 1.23 |
| β-cat-6 | 79.77 | 0.4 | 100.33 | 3.42 | 1.26 | 80.93 | 7.49 | 104.58 | 1.06 | 1.29 | 80.34 | 2.67 | 122.28 | 2.67 | 1.52 | 1.68 |
| β-catΔ-6 | 59.54 | 1.60 | 64.93 | 1.10 | 1.09 | 51.53 | 3.31 | 44.11 | 1.36 | 0.86 | 53.87 | 0.07 | 39.16 | 0.06 | 0.73 | 0.81 |

**Table S4.** Raw data from flow cytometry analysis for the β-catenin-responsive devices (Fig. 2F). For each device, the average relative fluorescence units (RFU) is shown along with the standard deviation (Stdev) between each duplicate sample. For each device the fold change in GFP expression and the fold change in the ratio of exon 7 excluded isoform levels to exon 7 included isoform levels (Excl/incl) (as determined by qRT-PCR analysis at 48 h; Fig. 2F and Fig. S2C) in the presence and absence of ligand are shown.

| **Position** | | | | | | | | | | | | |
|---|---|---|---|---|---|---|---|---|---|---|---|---|
| **3 (MS2)** | WTapt | | | WTapt | | | MUTapt | | | MUTapt | | |
| **10 (MS2)** | WTapt | | **Expression** | MUTapt | | **Expression** | WTapt | | **Expression** | MUTapt | | **Expression** |
| | **Avg. RFU** | **Stdev.** | **(fold)** | **Avg. RFU** | **Stdev.** | **(fold)** | **Avg. RFU** | **Stdev.** | **(fold)** | **Avg. RFU** | **Stdev.** | **(fold)** |
| **DsRed** | 17.17 | 0.74 | 1.00 | 26.73 | 2.26 | 1.00 | 21.47 | 1.92 | 1.00 | 35.44 | 2.18 | 1.00 |
| **MS2-DsRed** | 37.07 | 1.48 | 2.16 | 44.59 | 0.91 | 1.67 | 31.90 | 0.28 | 1.49 | 36.08 | 2.45 | 1.02 |

**Table S5.** Raw data from flow cytometry analysis for the MS2 multi-input processing regulatory device (Fig. 3B). For each device, the average relative fluorescence units (RFU) is shown along with the standard deviation (Stdev) between each duplicate sample and the fold change in GFP expression relative to the absence of ligand (DsRed only).

| **Position** | | | | | | | | | | | | |
|---|---|---|---|---|---|---|---|---|---|---|---|---|
| **3 (p50)** | WTapt | | | WTapt | | | MUTapt | | | MUTapt | | |
| **10 (MS2)** | WTapt | | Expression | MUTapt | | Expression | WTapt | | Expression | MUTapt | | Expression |
| | Avg. RFU | Stdev. | (fold) | Avg. RFU | Stdev. | (fold) | Avg. RFU | Stdev. | (fold) | Avg. RFU | Stdev. | (fold) |
| **DsRed** | 4.34 | 0.03 | 1.00 | 18.59 | 1.31 | 1.00 | 5.06 | 0.00 | 1.00 | 18.21 | 0.56 | 1.00 |
| **TNF-α** | 3.99 | 0.30 | 0.92 | 11.73 | 1.36 | 0.63 | 6.92 | 0.66 | 1.37 | 27.73 | 0.57 | 1.52 |
| **MS2-DsRed** | 6.91 | 0.16 | 1.59 | 13.94 | 0.33 | 0.75 | 10.05 | 0.00 | 1.99 | 13.39 | 0.76 | 0.74 |
| **TNF-α + DsRed** | 5.96 | 0.21 | 1.37 | 17.90 | 1.85 | 0.96 | 11.75 | 0.37 | 2.32 | 20.05 | 2.18 | 1.10 |
| **TNF-α + MS2-DsRed** | 22.93 | 1.11 | 5.28 | 11.30 | 0.23 | 0.61 | 13.39 | 0.76 | 2.65 | 18.86 | 1.23 | 1.04 |

**Table S6.** Raw data from flow cytometry analysis for the MS2 / NF-κB p50 multi-input processing regulatory device (Fig. 3D). For each device, the average relative fluorescence units (RFU) is shown along with the standard deviation (Stdev) between each duplicate sample and the fold change in GFP expression relative to the absence of ligand (DsRed only).

| Name | Primer sequence (5’ to 3’) |
|---|---|
| Ex6 | GCGCGCTAGCATGTATTATATGGTAAGTAATCACTCAGC |
| Ex8 | ATAGCTAGCGCTGCTACCTGCCAGC |
| GFP1 | GCGCGCTAGCGTGAGCAAGGGCGAG |
| GFP2 | GCGCGGGCCCTTAGTACAGCTCGTCCATGCC |
| Puma1 | ATAGTTTAAACGGTGGTTCT GGTGGTTCTGCCCGCGCACGCCAGGAG |
| Puma2 | GCGC GTTTAAACTTAATTGGGCTCCATCTCGGG |
| TK1 | GCGCGCTAGCGTGACAGGGGGAATGGC |
| TK2 | GCGCGTTTAAACTTAGTTAGCCTCCCCCATCTC |
| DsRed1 | ATAGGATCCGACAACACCGAGGACGTCAT |
| DsRed2 | ATAGCGGCCGCCTACTGGGAGCCGGAG |
| MS2-1 | AGCCAAAAAAAAAACGCAAAGTGGCTTCTAACTTTACTCAGTTCGTTC |
| MS2-2 | ATAGGATCCACCACCACCACCGTAGATGCCG |
| MS2-3 | ATAGGTACCATGGATTACAAGGATGACGATGACAAGCCAAAAAAAAAAC GCAAAGTGGCTTCTAACTTTAC |
| P50-1 | AGCCAAAAAAAAAACGCAAAGTGGCAGAAGATGATCCATATTTGGGAAG |
| P50-2 | ATAGGTACCGTCATCACTTTTGTCACAACCTTC |
| P50-3 | ATAGCTAGCATGGATTACAAGGATGACGATGACAAGCCAAAAAAAAAAC GCAAAGTGGCAGAAGATGATCC |
| SMN1cDNA | TAGAAGGCACAGTCGAGG |
| Bcat3 | ATATGATACTAGCTATCAGGCCGA |
| Bcat3Δ | ATATGATATCTAGCTATCTCGGTTAG |
| Bcat6 | ATATATCGATGTCTATATAGCTATTTTTTTTAACTT |
| Bcat6Δ | ATATATCGATGTCTATATAGCTATTTTTTTTAACTT |
| AptRv | ATACTCGAGCAGACTTACTCCTTAATTTAAGGAATG |

| | |
|---|---|
| p50(1) | ATATGATATCTAGCTATCCGCGC |
| p50(1)Δ | ATATGATATCTAGCTATCCGTAGCC |
| p50(2) | ATATGATATCTAGCTATCCGCGC |
| p65 | ATATGATATCTAGCTATCGAAGCTACAAGAAGGACAGCAC |

**Table S7.** Primer sequences used in this work.

| Name | Description |
|---|---|
| pCS1773 | SM1-GFP. Contains the wild-type SMN1 mini-gene fused to the C-terminus of GFP. |
| pCS1774 | SMN1 mini-gene template |
| pCS1775 | β-cat-3-GFP. Wild-type SMN1 mini-gene containing the β-catenin aptamer in position 3 of intron 6 fused to the C-terminus of GFP. |
| pCS1776 | β-catΔ-3-GFP. Wild-type SMN1 mini-gene containing the mutant β-catenin aptamer in position 3 of intron 6 fused to the C-terminus of GFP. |
| pCS1777 | β-cat-6-GFP. Wild-type SMN1 mini-gene containing the β-catenin aptamer in position 6 of intron 6 fused to the C-terminus of GFP. |
| pCS1778 | β-catΔ-6-GFP. Wild-type SMN1 mini-gene containing the mutant β-catenin aptamer in position 6 of intron 6 fused to the C-terminus of GFP. |
| pCS1779 | NF-κBp50(1)-3-GFP. Wild-type SMN1 mini-gene containing the NF-κBp50(1) aptamer in position 3 of intron 6 fused to the C-terminus of GFP. |
| pCS1780 | NF-κBp50(1) Δ-3-GFP. Wild-type SMN1 mini-gene containing the mutant NF-κBp50(1) aptamer in position 3 of intron 6 fused to the C-terminus of GFP. |
| pCS1781 | NF-κBp50(2)-3-GFP. Wild-type SMN1 mini-gene containing the NF-κBp50(2) aptamer in position 3 of intron 6 fused to the C-terminus of GFP. |
| pCS1782 | NF-κBp65-3-GFP. Wild-type SMN1 mini-gene containing the NF-κBp65 aptamer in position 3 of intron 6 fused to the C-terminus of GFP. |
| pCS1783 | NF-κBp65 Δ-3-GFP. Wild-type SMN1 mini-gene containing the mutant NF-κBp65 aptamer in position 3 of intron 6 fused to the C-terminus of GFP. |
| pCS1784 | MS2-3-MS2-10. Wild-type SMN1 mini-gene containing the MS2 aptamer in position 3 of intron 6 and in position 10 of intron 7 fused to the C-terminus of GFP. |
| pCS1785 | MS2Δ-3-MS2-10. Wild-type SMN1 mini-gene containing the mutant MS2 aptamer in position 3 of intron 6 and the wild-type MS2 aptamer in position 10 of intron 7 fused to the C-terminus of GFP. |
| pCS1786 | MS2-3-MS2Δ-10. Wild-type SMN1 mini-gene containing the wild-type MS2 aptamer in position 3 of intron 6 and the mutant MS2 aptamer in position 10 of |

| | |
|---|---|
| | intron 7 fused to the C-terminus of GFP. |
| pCS1787 | MS2Δ-3-MS2Δ-10. Wild-type SMN1 mini-gene containing the mutant MS2 aptamer in position 3 of intron 6 and in position 10 of intron 7 fused to the C-terminus of GFP. |
| pCS1788 | NF-κBp65-3-MS2-10. Wild-type SMN1 mini-gene containing the NF-κBp65 aptamer in position 3 of intron 6 and the MS2 aptamer in position 10 of intron 7 fused to the C-terminus of GFP. |
| pCS1789 | NF-κBp65Δ-3-MS2-10. Wild-type SMN1 mini-gene containing the mutant NF-κBp65 aptamer in position 3 of intron 6 and the MS2 aptamer in position 10 of intron 7 fused to the C-terminus of GFP. |
| pCS1790 | NF-κBp65-3-MS2Δ-10. Wild-type SMN1 mini-gene containing the NF-κBp65 aptamer in position 3 of intron 6 and the mutant MS2 aptamer in position 10 of intron 7 fused to the C-terminus of GFP. |
| pCS1791 | NF-κBp65Δ-3-MS2Δ-10. Wild-type SMN1 mini-gene containing the mutant NF-κBp65 aptamer in position 3 of intron 6 and the mutant MS2 aptamer in position 10 of intron 7 fused to the C-terminus of GFP. |
| pCS1792 | Puma. Contains *Puma* in pcDNA5/FRT. |
| pCS1793 | MS2-3. Wild-type SMN1 mini-gene containing the MS2 aptamer in position 3 of intron 6 fused to the C-terminus of GFP. |
| pCS1794 | MS2Δ-3. Wild-type SMN1 mini-gene containing the mutant MS2 aptamer in position 3 of intron 6 fused to the C-terminus of GFP. |
| pCS1795 | MS2-3-Puma. Wild-type SMN1 mini-gene containing the MS2 aptamer in position 3 of intron 6 fused to the C-terminus of Puma. |
| pCS1796 | MS2Δ-3-Puma. Wild-type SMN1 mini-gene containing the mutant MS2 aptamer in position 3 of intron 6 fused to the C-terminus of Puma. |
| pCS1797 | β-cat-6-Puma. Wild-type SMN1 mini-gene containing the β-catenin aptamer in position 6 of intron 6 fused to the C-terminus of Puma. |
| pCS1798 | β-catΔ-6-Puma. Wild-type SMN1 mini-gene containing the mutant β-catenin aptamer in position 6 of intron 6 fused to the C-terminus of Puma. |
| pCS1799 | p65-3-Puma. Wild-type SMN1 mini-gene containing the NF-κB p65 aptamer in position 3 of intron 6 fused to the C-terminus of Puma. |

| | |
|---|---|
| pCS1800 | p65Δ-3-Puma. Wild-type SMN1 mini-gene containing the mutant NF-κB p65 aptamer in position 3 of intron 6 fused to the C-terminus of Puma. |
| pCS1801 | HSV-TK. Contains *HSV-TK* in pcDNA5/FRT. |
| pCS1802 | β-cat-6-TK. Wild-type SMN1 mini-gene containing the β-catenin aptamer in position 6 of intron 6 fused to the C-terminus of HSV-TK. |
| pCS1803 | β-catΔ-6-TK. Wild-type SMN1 mini-gene containing the mutant β-catenin aptamer in position 6 of intron 6 fused to the C-terminus of HSV-TK. |
| pCS1804 | p65-3-TK. Wild-type SMN1 mini-gene containing the NF-κB p65 aptamer in position 3 of intron 6 fused to the C-terminus of HSV-TK. |
| pCS1805 | p65Δ-3-TK. Wild-type SMN1 mini-gene containing the mutant NF-κB p65 aptamer in position 3 of intron 6 fused to the C-terminus of HSV-TK. |
| pCS1392 | MS2-DsRed. Contains the FLAG-NLS-MS2 gene fused to the C-terminus of DsRed. |
| pCS1806 | NF-κBp50-DsRed. Contains the FLAG-NLS-NF-κBp50 gene fused to the C-terminus of DsRed. |
| pCS1807 | MS2-Venus. Contains the FLAG-NLS-MS2 gene fused to the C-terminus of Venus. |
| pCS1808 | Venus. Contains *Venus* in pcDNA5/FRT. |

**Table S8.** Plasmid constructs used in this work.

| **Name** | **Position** | **Restriction sites** | **Cassette (5'-3')** |
|---|---|---|---|
| MS2-1 | 1 | Kpn I/Cla I | ATATGGTACCAACA*CGTACACCATCAGGGTACG*TCCATATAAAGCTATAGATATCTAGCTATCGATATAT |
| MS2Δ-1 | 1 | Kpn I/Cla I | ATATGGTACCAACA*CGTACCCATCAGGGTACG*TCCATATAAAGCTATAGATATCTAGCTATCGATATAT |
| MS2-2 | 2 | Kpn I/Cla I | ATATGGTACCAACATCCATATAAAGCTAT*CGTACACCATCAGGGTACG*AGATATCTAGCTATCGATTAT |
| MS2Δ-2 | 2 | Kpn I/Cla I | ATATGGTACCAACATCCATATAAAGCTAT*CGTACCCATCAGGGTACG*AGATATCTAGCTATCGATTAT |
| MS2-3 | 3 | Eco RV/Xho I | ATATGATATCTAGCTATC*CGTACACCATCAGGGTACG*GATGTCTATATAGCTATTTTTTTTAACTTCCTTTATTTTCCTTACAGGGTTTCAGACAAAATCAAAAAGAAGGAAGGTGCTCACATTCCTTAAATTAAGGAGTAAGTCTGCTCGAGATAT |
| MS2Δ-3 | 3 | Eco RV/Xho I | ATATGATATCTAGCTATC*CGTACCCATCAGGGTACG*GATGTCTATATAGCTATTTTTTTTAACTTCCTTTATTTTCCTTACAGGGTTTCAGACAAAATCAAAAAGAAGGAAGGTGCTCACATTCCTTAAATTAAGGAGTAAGTCTGCTCGAGATAT |
| MS2-4 | 4 | Cla I/Xho I | ATATATCGATGTCTATATAGCT*CGTACACCATCAGGTACG*ATTTTTTTTAACTTCCTTTATTTTCCTTACAGGGTTTCAGACAAAATCAAAAAGAAGGAAGGTGCTCACATTCCTTAAATTAAGGAGTAAGTCTGCTCGAGATAT |
| MS2Δ-4 | 4 | Cla I/Xho I | ATATATCGATGTCTATATAGCT*CGTACCCATCAGGGTACG*ATTTTTTTTAACTTCCTTTATTTTCCTTACAGGGTTTCAGACAAAATCAAAAAGAAGGAAGGTGCTCACATTCCTTAAATTAAGGAGTAAGTCTGCTCGAGATAT |
| MS2-5 | 5 | Cla I/Xho I | ATATATCGATGTCTATATAGCTATTTTTTTTAACTTC*CGTACACCATCAGGGTACG*CTTTATTTTCCTTACAGGGTTTCAGACAAAATCAAAAAGAAGGAA |

| | | | |
|---|---|---|---|
| | | | GGTGCTCACATTCCTTAAATTAAGGAGTAAGTC TGCTCGAGATAT |
| MS2Δ-5 | 5 | Cla I/Xho I | ATATATCGATGTCTATATAGCTATTTTTTTTAAC TTC*CGTACCCATCAGGGTACG*CTTTATTTTCCTTA CAGGGTTTCAGACAAAATCAAAAAGAAGGAAG GTGCTCACATTCCTTAAATTAAGGAGTAAGTCT GCTCGAGATAT |
| MS2-6 | 6 | Cla I/Xho I | ATATATCGATGTCTATATAGCTATTTTTTTTAAC TTCCTTTATTTTCCTTAC*CGTACACCATCAGGGTA CG*AGGGTTTCAGACAAAATCAAAAAGAAGGAA GGTGCTCACATTCCTTAAATTAAGGAGTAAGTC TGCTCGAGATAT |
| MS2Δ-6 | 6 | Cla I/Xho I | ATATATCGATGTCTATATAGCTATTTTTTTTAAC TTCCTTTATTTTCCTTAC*CGTACCCATCAGGGTAC G*AGGGTTTCAGACAAAATCAAAAAGAAGGAAG GTGCTCACATTCCTTAAATTAAGGAGTAAGTCT GCTCGAGATAT |
| MS2-7 | 7 | Cla I/Xho I | ATATATCGATGTCTATATAGCTATTTTTTTTAAC TTCCTTTATTTTCCTTACAGGGTTTCAGACAAAA TCAAAAAGAAGGAAGGTGCTCACATTCCTTAAA TTAAGGAGTAAGTCTG*CGTACACCATCAGGGTAC G*CTCGAGATAT |
| MS2Δ-7 | 7 | Cla I/Xho I | ATATATCGATGTCTATATAGCTATTTTTTTTAAC TTCCTTTATTTTCCTTACAGGGTTTCAGACAAAA TCAAAAAGAAGGAAGGTGCTCACATTCCTTAAA TTAAGGAGTAAGTCTG*CGTACCCATCAGGGTACG* CTCGAGATAT |
| MS2-8 | 8 | Xho I/HindIII | ATATCTCGAGCCAGCATTA*CGTACACCATCAGGG TACG*TGAAAGTGAATCTTACTTTTGTAAAAAAG CTTATAT |
| MS2Δ-8 | 8 | Xho I/HindIII | ATATCTCGAGCCAGCATTA*CGTACCCATCAGGGT ACG*TGAAAGTGAATCTTACTTTTGTAAAAAAGC TTATAT |
| MS2-9 | 9 | Xho I/HindIII | ATATCTCGAGCCAGCATTATGAAAGTGAATCTT A*CGTACACCATCAGGGTACG*CTTTTGTAAAAAAG CTTATAT |
| MS2Δ-9 | 9 | Xho I/HindIII | ATATCTCGAGCCAGCATTATGAAAGTGAATCTT |

| | | | |
|---|---|---|---|
| | | | A*CGTACCCATCAGGGTACG*CTTTTGTAAAAAAGC TTATAT |
| MS2-10 | 10 | Xho I/Bam HI | ATATCTCGAGCCAGCATTATGAAAGTGAATCTT ACTTTTGTAAAAAAGC*CGTACACCATCAGGGTAC G*TTCTTTATGGTTTGTGGGATCCATAT |
| MS2Δ-10 | 10 | Xho I/Bam HI | ATATCTCGAGCCAGCATTATGAAAGTGAATCTT ACTTTTGTAAAAAAGC*CGTACCCATCAGGGTACG* TTCTTTATGGTTTGTGGGATCCATAT |
| MS2-11 | 11 | HindIII/Bam HI | ATATAAGCTTCTTTATGGTTTGT*CGTACACCATC AGGGTACG*GGGATCCATAT |
| MS2Δ-11 | 11 | HindIII/Bam HI | ATATAAGCTTCTTTATGGTTTGT*CGTACCCATCA GGGTACGG*GGGATCCATAT |
| MS2-12 | 12 | Bam HI/Xba I | ATATGGATCCAAATGTTT*CGTACACCATCAGGGT ACG*TTGAACAGTTAATCTAGAATAT |
| MS2Δ-12 | 12 | Bam HI/Xba I | ATATGGATCCAAATGTTT*CGTACCCATCAGGGTA CG*TTGAACAGTTAATCTAGAATAT |
| β-cat-3 | 3 | Eco RV/Xho I | ATATGATATCTAGCTATC*AGGCCGATCTATGGAC GCTATAGGCACACCGGATACTTTAACGATTGGCT*G ATGTCTATATAGCTATTTTTTTTAACTTCCTTTA TTTTCCTTACAGGGTTTCAGACAAAATCAAAAA GAAGGAAGGTGCTCACATTCCTTAAATTAAGGA GTAAGTCTGCTCGAGATAT |
| β-catΔ-3 | 3 | Eco RV/Xho I | ATATGATATCTAGCTATC*TCGGTTAGCAATTTCAT AGGCCACACGGATATCGCAGGTATCTAGCCGGA*G ATGTCTATATAGCTATTTTTTTTAACTTCCTTTA TTTTCCTTACAGGGTTTCAGACAAAATCAAAAA GAAGGAAGGTGCTCACATTCCTTAAATTAAGGA GTAAGTCTGCTCGAGATAT |
| β-cat-6 | 6 | Cla I/Xho I | ATATATCGATGTCTATATAGCTATTTTTTTTAAC TTCCTTTATTTTCCTTAC*AGGCCGATCTATGGACG CTATAGGCACACCGGATACTTTAACGATTGGCT*AG GGTTTCAGACAAAATCAAAAAGAAGGAAGGTG CTCACATTCCTTAAATTAAGGAGTAAGTCTGCT CGAGATAT |

| | | | |
|---|---|---|---|
| β-catΔ-6 | 6 | Cla I/Xho I | ATATATCGATGTCTATATAGCTATTTTTTTTAAC TTCCTTTATTTTCCTTAC*TCGGTTAGCAATTTCATA GGCCACACGGATATCGCAGGTATCTAGCCGGA*AG GGTTTCAGACAAAATCAAAAAGAAGGAAGGTG CTCACATTCCTTAAATTAAGGAGTAAGTCTGCT CGAGATAT |
| NF-κBp50(1)-3 | 3 | Eco RV/Xho I | ATATGATATCTAGCTATC*GCATCCTGAAACTGTTT TAAGGTTGGCCGATGC*GATGTCTATATAGCTATT TTTTTTAACTTCCTTTATTTTCCTTACAGGGTTTC AGACAAAATCAAAAAGAAGGAAGGTGCTCACA TTCCTTAAATTAAGGAGTAAGTCTGCTCGAGAT AT |
| NF-κBp50(1)Δ-3 | 3 | Eco RV/Xho I | ATATGATATCTAGCTATC*CGTAGCCGGTTGGAAT TTTGTCAAAGTCCTACG*GATGTCTATATAGCTATT TTTTTTAACTTCCTTTATTTTCCTTACAGGGTTTC AGACAAAATCAAAAAGAAGGAAGGTGCTCACA TTCCTTAAATTAAGGAGTAAGTCTGCTCGAGAT AT |
| NF-κBp50(2)-3 | 3 | Eco RV/Xho I | ATATGATATCTAGCTATCCGCGC*GATCTTGAAAC TGTTTTAAGGTTGGCCGAT*CGCGCGGATGTCTAT ATAGCTATTTTTTTTAACTTCCTTTATTTTCCTTA CAGGGTTTCAGACAAAATCAAAAAGAAGGAAG GTGCTCACATTCCTTAAATTAAGGAGTAAGTCT G CTCGAGATAT |
| NF-κBp65-3 | 3 | Eco RV/Xho I | *GAAGCTTACAAGAAGGACAGCACGAATAAAACCTG CGTAAATCCGCCCCATTTGTGTAAGGGTAGTGGGT CGAATTCCGCTCA*GATGTCTATATAGCTATTTTTT TTAACTTCCTTTATTTTCCTTACAGGGTTTCAGA CAAAATCAAAAAGAAGGAAGGTGCTCACATTC CTTAAATTAAGGAGTAAG |
| NF-κBp65Δ-3 | 3 | Eco RV/Xho I | *ACTCGCCTTAAGCTGGGTGATGGGAATGTGTTTAC CCCGCCTAAATGCGTCCAAAATAAGCACGACAGGA AGAACATTCGAAG*GATGTCTATATAGCTATTTTTT TTAACTTCCTTTATTTTCCTTACAGGGTTTCAGA CAAAATCAAAAAGAAGGAAGGTGCTCACATTC CTTAAATTAAGGAGTAAG |

**Table S9.** Aptamer cassette sequences used in the construction of the RNA devices. Aptamer sequences are italicized and nucleotides added for strengthening aptamer secondary structure are in red.

| Name | Forward Primer (5’ - 3’) | Reverse Primer (5’ - 3’) | Isoform |
|---|---|---|---|
| Pair 1 | GTATTATATGGAAATGCTGG | GAA GGTGGTCACGAGGG | Ex6/8 and GFP |
| Pair 2 | TAAATTAAGGAGAAATGCT | GAA GGTGGTCACGAGGG | Ex7/8 and GFP |
| Pair 3 | CAAAGATGGTCAAGGTCGCAAG | GGCGATGTCAATAGGACTCC | HPRT |

**Table S10.** Primer sequences for transcript isoform analysis through qRT-PCR.

**References and Notes**


S1. S. J. Culler, K. G. Hoff, R. B. Voelker, J. A. Berglund, C. D. Smolke, *Nucleic Acids Res* **38,** 5152 (Aug, 2010).
S2. K. Stade, C. S. Ford, C. Guthrie, K. Weis, *Cell* **90**, 1041 (Sep 19, 1997).
S3. J. Villemaire, I. Dion, S. A. Elela, B. Chabot, *J Biol Chem* **278**, 50031 (Dec 12, 2003).
S4. J. Carey, P. T. Lowary, O. C. Uhlenbeck, *Biochemistry* **22**, 4723 (Sep 27, 1983).
S5. H. K. Lee, Y. S. Choi, Y. A. Park, S. Jeong, *Cancer Res* **66**, 10560 (Nov 1, 2006).
S6. R. Chan *et al.*, *Nucleic Acids Res* **34**, e36 (2006).
S7. J. Mi *et al.*, *Nucleic Acids Res* **34**, 3577 (2006).
S8. S. E. Wurster, L. J. Maher, 3rd, *Rna* **14**, 1037 (Jun, 2008).
S9. B. R. Graveley, K. J. Hertel, T. Maniatis, *Embo J* **17**, 6747 (Nov 16, 1998).
S10. R. G. Chubet, B. L. Brizzard, *Biotechniques* **20**, 136 (Jan, 1996).
S11. D. Kalderon, B. L. Roberts, W. D. Richardson, A. E. Smith, *Cell* **39**, 499 (Dec, 1984).
S12. L. A. Cassiday, L. J. Maher, 3rd, *Proc Natl Acad Sci U S A* **100**, 3930 (Apr 1, 2003).
S13. T. Nagai *et al.*, *Nat Biotechnol* **20**, 87 (Jan, 2002).
S14. C. E. Hellweg, A. Arenz, S. Bogner, C. Schmitz, C. Baumstark-Khan, *Ann N Y Acad Sci* **1091**, 191 (Dec, 2006).
S15. M. Mezhybovska, K. Wikstrom, J. F. Ohd, A. Sjolander, *J Biol Chem* **281**, 6776 (Mar 10, 2006).
S16. K. J. Livak, T. D. Schmittgen, *Methods* **25**, 402 (Dec, 2001).
S17. Y. Y. Chen, M. C. Jensen, C. D. Smolke, *Proc Natl Acad Sci U S A* **107**, 8531 (May 11, 2010).
S18. J. Sinha, S. J. Reyes, J. P. Gallivan, *Nat Chem Biol* **6**, 464 (Jun, 2010).
S19. L. Du, R. A. Gatti, *Curr Opin Mol Ther* **11**, 116 (Apr, 2009).
S20. L. Cartegni, A. R. Krainer, *Nat Struct Biol* **10**, 120 (Feb, 2003).
S21. L. A. Skordis, M. G. Dunckley, B. Yue, I. C. Eperon, F. Muntoni, *Proc Natl Acad Sci U S A* **100**, 4114 (Apr 1, 2003).
S22. D. Gendron *et al.*, *BMC Biotechnol* **6**, 5 (2006).
S23. X. Jiang *et al.*, *Biochem Biophys Res Commun* **301**, 583 (Feb 7, 2003).
S24. D. B. Huang *et al.*, *Proc Natl Acad Sci U S A* **100**, 9268 (Aug 5, 2003).
S25. A. R. Buskirk, D. R. Liu, *Chem Biol* **12**, 151 (Feb, 2005).